

**PERFORMANCE OPTIMIZATION OF SOLAR PV SYSTEM OVER
THE GAPS OF THE MODULE AND ROOF FOR EFFECTIVE
VENTILATION**

DOMINIC YEOW ZONG HUI


**A project report submitted in partial fulfilment of the
requirements for the award of Bachelor of Engineering
(Honours) Electrical and Electronics Engineering**

**Lee Kong Chian Faculty of Engineering and Science
Universiti Tunku Abdul Rahman**

June 2020

DECLARATION

I hereby declare that this project report is based on my original work except for citations and quotations which have been duly acknowledged. I also declare that it has not been previously and concurrently submitted for any other degree or award at UTAR or other institutions.

Signature : 

Name : Dominic Yeow Zong Hui


ID No. : 15UEB01315

Date : 5 October 2020

APPROVAL FOR SUBMISSION

I certify that this project report entitled “**PERFORMANCE OPTIMIZATION OF SOLAR PV SYSTEM OVER THE GAPS OF THE MODULE AND ROOF FOR EFFECTIVE VENTILATION**” was prepared by **DOMINIC YEOW ZONG HUI** has met the required standard for submission in partial fulfilment of the requirements for the award of Bachelor of Engineering (Honours) Electrical and Electronics Engineering at Universiti Tunku Abdul Rahman.

Approved by,

Signature : 

Supervisor : Ir. Dr. Lim Boon Han

Date : 30 Sep 2020

The copyright of this report belongs to the author under the terms of the copyright Act 1987 as qualified by Intellectual Property Policy of Universiti Tunku Abdul Rahman. Due acknowledgement shall always be made of the use of any material contained in, or derived from, this report.

© 2020, Dominic Yeow Zong Hui. All right reserved.

ACKNOWLEDGEMENTS

First, I would like to thank Universiti Tunku Abdul Rahman (UTAR) for allowing me to conduct this project so that I can use the skills gotten through study. UTAR not only provided me with well-equipped laboratory facilities, but also provide me with a convenient location to conduct projects.

Besides that, I would also like to express my greatest gratitude to my supervisor Ir. Dr. Lim Boon Han who has given me many suggestions on how to conduct research and experiment projects professionally. He gives me suggestion on conduct research on related project and provide me with guidance when encounter problems at projects.

Finally, I would also like to thanks to my friends and students whose projects under my supervisor helped me completing the research experimental projects within the timetable. They have provided so much support and guidance during my research experimental project.

ABSTRACT

The performance of a solar photovoltaic (PV) module drops by 0.35 %/°C to 0.4 %/°C as compared its power rating measured as 25 °C under standard test condition (STC). In the tropics, PV array installed as a building-attached photovoltaic (BAPV) system experiences high module temperature because 1) the ambient temperature is high. 2) heat of the rear side of the panel cannot be dissipated effectively through convection because the air gap between the rear side of the solar panel and roof is narrow. Therefore, a cheaper solution purpose in this project is to increase the air gap distance by changing the dimension of the existing mechanical supports to promote a better air ventilation to reduce the operating temperature of the solar panel. However, there is lack of research on the optimal air gap distance that can give the optimal cost- effective solution for BAPV systems operating in the tropics. Therefore, it is essential to model the performance improvement via ventilation by changing the air gap distance so that the optimal air gap can be proposed for the industry. In this project, I model and analyze, the effects of how the air gap between the solar panels and metal deck roof affects the performance of the PV panel.

The experiment was done by setting up two commercial PV panels in a side by-side configuration. One PV panel has fixed air gap of 12.5 cm in between the panel and the metal deck roof and another one panel was installed in such a way that the air gap distance can be adjusted. Eight DS18B20 temperature sensors were calibrated before attaching at the back of both PV panels. A Raspberry Pi electronic board was programmed as a temperature data logger. The two PV panels were calibrated under the same condition, with the same air gap distance and connected to the same micro-inverter. The experiment was started with adjustment of the air gap distance of 10.5 cm and measurement were carried for 5 days. The subsequent experiment was to increase the air gap by 2 cm and with the same interval of measurement. The experiment was repeated up to an air gap distance of 20.5 cm. The temperature of the PV panel under different air gap distances were compared. Besides, the electricity output of both panels was compared and analysed.

As the result, as the air gap increased from 12.5 cm to 20.5 cm, the overall average operating temperature of the PV panel relatively to reference PV panel

decrease to 1.5 °C, thereby increase the total electricity generation percentage to 1.3 %. The Ross coefficient value had decreased from 0.0246 °C m²/W to 0.0166 °C m²/W. Hence, it proves that natural ventilation plays a huge role in dissipating the heat of PV panels, which will then increase the electricity generation of the PV panels. Finally, a cost analysis was performed to calculate the extra income can be obtained from electricity selling and the additional cost of the mechanical air gaps from the increment of air gap distance. It shows that for air gap distance of 20.5 cm, a PV system of 90 kW can gain extra energy profit of RM 21140.87 through 21 years of project lifetime under Net Energy Metering (NEM) scheme available in Malaysia.

TABLE OF CONTENTS

DECLARATION		i
APPROVAL FOR SUBMISSION		ii
ACKNOWLEDGEMENTS		iv
ABSTRACT		v
TABLE OF CONTENTS		vii
LIST OF TABLES		x
LIST OF FIGURES		xii
LIST OF SYMBOLS / ABBREVIATIONS		xv
LIST OF APPENDICES		xvi
 CHAPTER		
1	INTRODUCTION	1
	1.1 General Introduction	1
	1.2 Problem Statement	2
	1.3 Aim and Objectives	2
	1.4 Importance of the Study	3
	1.5 Scope and Limitation of the Study	3
	1.6 Contribution of the Study	4
	1.7 Outline of the Report	4
2	LITERATURE REVIEW	5
	2.1 Effect of Temperature on the PV Panel	5
	2.2 Past Research of Effect or Optimization for Ventilation on BAPV System	10
	2.2.1 Optimization of Air Gap for Ventilation on BAPV System by Simulation	10
	2.2.2 Effect of Air Gap and Type of Roof on Temperature at BAPV system based on Malaysia Climate	12
	2.2.3 Effect of Inclination Angle and Type of Roof on Temperature at BAPV system based on Malaysia Climate	14

	2.2.4	Effect of Inclination Angle and Air Gap on Temperature of BAPV system based on Malaysia Climate	17
	2.2.5	Effect of Forced Convection on Temperature of BAPV system based on Malaysia Climate	19
	2.3	Summary	22
3		METHODOLOGY AND WORK PLAN	23
	3.1	Experimental Setup	23
	3.1.1	Metal Deck and PV System Setup	25
	3.1.2	Raspberry PI 3 Temperature Data Logger	26
	3.2	Apparatuses & Instrument	28
	3.2.1	Poly-crystalline PV panels	28
	3.2.2	Raspberry Pi 3 Model B +	29
	3.2.3	DS18B20 Temperature Sensors	30
	3.2.4	AP System YC500 Micro-Inverter	30
	3.3	Overall Project Procedure	31
	3.4	Experimental Preparation	33
	3.4.1	Temperature Sensors Calibration	33
	3.4.2	PV Panels Calibration	36
	3.5	Experimental Measurement	39
	3.6	Experimental Analysis	40
	3.6.1	PV Average Temperature Analysis	40
	3.6.2	PV Electricity Generation Analysis	42
	3.6.3	Ross Coefficient Analysis	43
	3.6.4	Cost Analysis	43
	3.7	Experimental Planning	46
	3.8	Summary	49
4		RESULTS AND DISCUSSION	50
	4.1	Introduction	50
	4.2	Average Temperature Analysis	50
	4.3	Electricity Generation Analysis	53
	4.4	Ross Coefficient Analysis	57
	4.5	Cost Analysis	61
	4.6	Summary	64

5	CONCLUSIONS AND RECOMMENDATIONS	66
5.1	Conclusions	66
5.2	Recommendations for future work	67
	REFERENCES	68

LIST OF TABLES

Table 2.1.1: Measured Temperature coefficient for Multi C-Si technologies. (Dash and Gupta, 2015)	7
Table 2.2.2.1: Table of Irradiance, Height and Temperature Difference between 4 Type of Configuration. (Zakaria et al., 2013)	19
Table 2.2.3.1: Summary of correlation on PV Cell Temperature versus Solar Irradiance in Different Roof Materials and Inclination angle. (Ho, 2015)	16
Table 2.2.3.2: Summary of correlation on Power Loss versus Solar Irradiance in Different Roof Materials and Inclination angle. (Ho, 2015)	16
Table 2.2.5.1: Summary of experimental fan configuration in BAPV system. (Chong, 2015)	20
Table 3.4.2.1: Result of Electricity Generation Calibration at an air gap of 12.5 cm.	39
Table 3.7.1: Gantt chart of the first half of the project.	47
Table 3.7.2: Planned Gantt chart of the second half of the project.	48
Table 4.2.1: Table of experimental air gap and operating temperature in the experiment PV panel relatively to reference PV panel, $\Delta T_{Avg,Acc}$	50
Table 4.2.2: Table of the experimental air gap and shifted operating temperature in the experimental PV panel relative to reference PV panel.	52
Table 4.3.1: Table of the experimental air gap, electricity generation by reference PV panel and theoretical experiment PV panel also electricity generation percentage difference between theoretical experimental PV panel and reference PV Panel, $\%E_{Theo}$.	54
Table 4.3.2: Table of the experimental air gap, electricity generation by reference PV panel and actual experiment PV panel also electricity generation percentage difference between actual experimental PV panel and reference PV Panel, $\%E_{Theo}$.	54
Table 4.3.3: Table of the experimental air gap and shifted electricity generation percentage increment between theoretical or actual experimental PV panel and reference PV Panel, $\%E_{Theo,inc}$.	56
Table 4.4.1: Table of experimental air gap, reference PV panel Ross coefficient value, k_{ref} and experimental PV panel Ross coefficient value, k_{Exp} .	58

Table 4.4.2: Table of the experimental air gap, Ross coefficient difference between experimental PV panel and reference PV panel, Δk , shifted Ross coefficient difference between experimental PV panel and reference PV panel, Δk_{shift} and final Ross coefficient value on experimental PV panel, k_f . 60

Table 4.5.1: Material Cost for aluminium hook and price increment per aluminium hook based on reference air gap. 61

Table 4.5.2: Table of experiment air gap and total price Investment on a 90 kW BAPV System. 62

Table 4.5.3: Table of experiment air gap, improved performance Ratio for a PV system, and extra electricity generation in a year. 63

Table 4.5.4: Table of experiment air gap, extra electricity generation in 21 years, and extra electricity income in 21 years. 63

LIST OF FIGURES

Figure 1.1.1: BAPV system on grid application in a home. (Salam et al., 2015)	1
Figure 2.1.1: Current-Voltage (I-V) Curve. (Amelia et al., 2016)	6
Figure 2.1.2: Power-Voltage (P-V) Curve. (Amelia et al., 2016)	6
Figure 2.1.3: Graph of PV Temperature Difference between Ambient and Module Temperature versus Irradiance Comparison between Singapore (P4), Germany, and Spain. (Ye et al., 2013)	9
Figure 2.2.1.1: Measurement of realistic PV Module (Type B485) with Air Gap Definition in CFD Simulation. (Gan, 2009b)	10
Figure 2.2.1.2: Graph of mean temperature versus air gap with varies roof pitch and solar irradiance for one solar panel from the result of CFD Simulation. (Gan, 2009b)	11
Figure 2.2.2.1: Metal-Deck roof Mock-Up Experiment in campus in Shah Alam, Selangor. (Zakaria et al., 2013)	12
Figure 2.2.2.2: Graph of Cell Temperature versus Ambient Temperature with Poly-Si, metal deck at different air gaps. (Zakaria et al., 2013)	14
Figure 2.2.3.1: Metal-Deck Roof Mock-Up Experiment in Bandar Sg Long, Selangor.(Ho, 2015)	15
Figure 2.2.4.1: Metal-Deck Roof Mock-Up Experiment in Bandar Sg Long, Selangor.(Chew, 2015)	17
Figure 2.2.4.2: Graph of PV Operating Temperature versus Solar Irradiance at various Air Gap with Zero slanting angle.(Chew, 2015)	18
Figure 2.2.5.1: BAPV system configuration setting with Air Gap and slanting angle definition. (Chong, 2015)	19
Figure 2.2.5.2: Fan System beneath BAPV system. (Chong, 2015)	20
Figure 3.1.1: Experimental Setup Block Diagram for determining the effect of the air gap for ventilation of BAPV systems.	23
Figure 3.1.2: Actual Setup Diagram to determine the effect of the air gap for ventilation of BAPV systems.	24
Figure 3.1.1.1: Sketching of Installation of Metal Deck.	25
Figure 3.1.1.2: Installation of Components on PV Panel.	26

Figure 3.1.2.1: Component used for Temperature Data logger.	27
Figure 3.1.2.2: Temperature Data Logger Breadboard Schematic Diagram.	27
Figure 3.2.1.1: Malaysian Solar Resources (MSR) model MYS-60P/B3/CF 260 polycrystalline PV panel.	29
Figure 3.2.2.1: Raspberry Pi Model 3 B+	29
Figure 3.2.3.1: DS18B20 Temperature Sensor (Left: Waterproof Module, Right: Transistor Type)	30
Figure 3.2.4.1: AP System YC500 micro-inverter.	31
Figure 3.3.1: Overall Research Procedure.	32
Figure 3.4.1.1: DS18B20 Waterproof Temperature Sensor Calibration by using Boiling Water.	33
Figure 3.4.1.2: Insertion of metal plate into Boiling Water for DS18B20 Temperature Sensor Calibration.	34
Figure 3.4.1.3: Attachment of DS18B20 Temperature Sensors onto beneath of PV panel.	35
Figure 3.4.2.1: Measurement of air gap distance between PV panel and metal deck roof.	36
Figure 3.4.2.1: Setting of Two PV panels side by side.	37
Figure 3.5.1: Table of measurement.	40
Figure 4.2.1: Graph of average operating temperature in the experiment PV panel relatively to the reference PV panel versus experimental air gap.	51
Figure 4.2.2: Graph of shifted average operating temperature in the experiment PV panel relatively to the reference PV panel versus experimental air gap.	53
Figure 4.3.1: Graph of Electricity Generation Percentage Difference Versus Experimental Air Gap.	56
Figure 4.4.1: Graph of ΔT_{PV} versus Solar Irradiance for Reference air gap = 12.5 cm and Experimental Air Gap= 12.5 cm.	57
Figure 4.4.2: Graph of Final Ross Coefficient Values versus Experimental Air Gap.	60
Figure 4.5.1: Graph of Extra Cost on a 90 kW BAPV system versus Experimental air gap.	62

Figure 4.5.2: Graph of extra Electricity Income in 21 years versus Experimental air gap. 64

LIST OF SYMBOLS / ABBREVIATIONS

β	Temperature coefficient of Voltage, %/°C
γ	Temperature coefficient of Power, %/°C
k	Ross coefficient that determine the slope between the temperature and irradiance level, °C m ² /W
d_f	Final air gap distance, cm
AC	Alternating Current
BAPV	Building Applied Photovoltaic
CFD	Computational Fluid Dynamics
DC	Direct Current
EMA	Energy Management Analysis
FiT	Feed-in Tariff
GPIO	General Purpose Input/Output
HDMI	High Definition Multimedia Interface
IoT	Internet of Things
MPPT	Maximum Point Power Tracking
MSR	Malaysian Solar Resources
NEM	Net Energy Metering
PV	Photovoltaics
PPA	Power Purchasing Agreement
PSH	Peak Sun Hour
SEA	South East Asia
SEDA	Sustainable Energy Development Authority
TNB	Tenaga National Berhad
STC	Standard Test Condition
USB	Universal Serial Bus
UTC	Universal Time Coordinated
UTAR	Universiti Tunku Abdul Rahman

LIST OF APPENDICES

APPENDIX A: Raspberry PI Data Logger Coding	71
APPENDIX B: List of result for Average Operating Temperature of PV Panels in A Day and Temperature Difference between reference PV panel and experimental PV panel	77
APPENDIX C: Result List for Electricity Generation by PV Panel in A Day and Electricity Generation Percentage Difference Between Reference PV panel and Experimental PV Panel.	80
APPENDIX D: List of Ross Coefficient Value Graphs between Experimental PV Panel and Reference PV Panel in different air gap.	82

CHAPTER 1

INTRODUCTION

1.1 General Introduction

Photovoltaic (PV) systems are an integration of PV modules, inverter, mounting rack, etc. This system converts solar energy directly into electricity. (Boyle, 2012). In recent years, the installation capacity of the PV system has increased around the world including Malaysia, which has reported by Renewable Global Status Report (REN21, 2019) and Malaysia Energy Statistics Handbook (Suruhanjaya Tenaga, 2019) . The increment of the installation of PV systems is driven by the introduction of Feed-in Tariff (FiT) and Net Energy Metering (NEM) policies provided by the government. There were several types of installation of PV systems and one type of the installation is called Building Applied PV (BAPV) systems.

BAPV system is defined as a photovoltaic module fastened or retrofitted onto the envelope of the building. (Berger et al., 2018; IEC/TS61836, 2016). BAPV system consists of PV array, combiner box, DC and AC switchgear, inverters, also electric energy meters. Figure 1.1.1 below shows an example of a BAPV system.

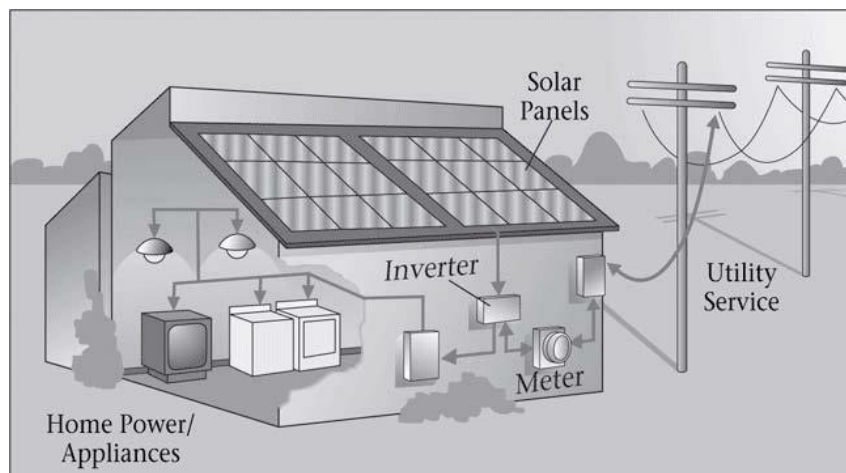


Figure 1.1.1: BAPV system on grid application in a home. (Salam et al., 2015)

Although the number of PV system installations in Malaysia has increased, the expectation for the number of BAPV system installations is still

low. This is because most building developers and consumers questioned the cost and reliability of PV system installed on the roof. (Goh et al., 2017). One aspect of reliability is the inconsistent power outputs of PV panels. One of the reasons is the operating temperature of solar cells. This fact is due to heat cannot dissipate effectively through convective cooling if a PV module is mounted flat on a roof. It is stated that if the operating temperature increase by 1 °C, the power output will be decreasing by 0.387% for the multi-crystalline PV panel. (Dash and Gupta, 2015)

Therefore, many solutions are proposed to reduce the PV module temperature for the BAPV systems such as the use of water-cooling or air-cooling systems. However, these solutions are expensive. Therefore, a cheaper solution purpose in this project is to increase the air gap distance by changing the dimension of the existing mechanical supports to promote a better air ventilation to reduce the operating temperature of the solar panel. This fact is because optimization of the air gap distance for natural convection will let the cost of the mechanical supporting structure of a BAPV system lesser also bring out of the maximum efficiency of BAPV systems as the operating temperature of the PV panel will decrease.

1.2 Problem Statement

The Problem statement of the research on air gap optimization for BAPV system is summarized as follow:

- It is well known that the increment of the air gap distance between a PV panel and the roof can contributes up to 50% of the benefits to achieve a lower module temperature in BAPV systems. (Ye et al., 2013). However, there is lack of research on the optimal air gap distance that can give the optimal cost-effective solution for BAPV systems operating in the tropics.

1.3 Aim and Objectives

The project aims to analyse, model, and optimize the air gap distance between solar PV panel and the metal deck on the performance of PV panel.

While the objectives of the project are:

1. To record the temperature of PV panels by using a data logger and temperature sensors at the different air gap distance between solar panel and metal deck roof.
2. To model the relationship between the ventilation of PV systems and the performance of the PV panel at different air gap distances between the solar panel and metal deck roof.
3. To obtain the optimal air gap through the modelling as a guidance for the industry practice to improve the performance of a PV system.

1.4 Importance of the Study

The result of this present study may provide guidance for installation BAPV system in tropical regions such as Malaysia. Besides that, the study also provides importance as below:

- Provide the insight to optimize the cost of the mechanical structure during installation in the BAPV system.
- Boost up the solar market industry as the efficiency of the BAPV system increase.

1.5 Scope and Limitation of the Study

The study focuses on reducing the temperature of the PV panels of the BAPV system by analysing the effect of the increasing the air gap distance between the PV panels and the roof. Besides that, it also focuses on determine the optimal air gap distance by analysing the correlation between the air gap and the metal deck roof versus the output of the PV system. The experiment was conducted on the roof of Universiti Tunku Abdul Rahman (UTAR) KB Block where located at Bandar Sungai Long City Campus in Kajang, Selangor, Malaysia. To achieve the above improvements, it is necessary to study and understand the temperature effects of the PV panels.

The limitations of this research are limited to one type of polycrystalline silicon PV panel and its system. The tilt angle of the roof is fixed to 10 degrees, regardless of another angle.

1.6 Contribution of the Study

The results of the study will provide references for the installation of the BAPV system in tropical regions such as Malaysia. In addition, the findings of the research will also optimize performance cost index for the BAPV system.

1.7 Outline of the Report

The report has separated into 5 chapters and the summary of the chapter is shown below:

Chapter 1 introduces the general introduction of the BAPV system, the problem faced by BAPV system which temperature effect on the PV panel and solutions for solving the temperature effects on the BAPV System which is increasing air gap distance between PV panel and metal deck had been stated. The first chapter also stated the problem statement and pointed out the project's goals. This chapter also explain the importance, scope and limitation and contribution of the research.

Chapter 2 focuses on the literature review of influence of temperature on PV panels, as well as previous research on the solution to reduce the influence of temperature on the PV panel.

Chapter 3 is focusing on the method such as set up of the BAPV system and Raspberry PI temperature data logger. Besides that, this chapter focuses on calibration of temperature sensors PV panels. In addition, this chapter will also focus on data measurement and data analysis method such as average temperature, electricity generation, Ross coefficient and cost-effectiveness.

Chapter 4 focuses on using the analysis methods in Chapter 3 to analyse, create and interpret results. Chapter 5 focuses on the drawing conclusion based on the results and making further recommendations for the research work.

CHAPTER 2

LITERATURE REVIEW

2.1 Effect of Temperature on the PV Panel

One of the problems that affects the efficiency of PV panels is the operating temperature around the PV panels because solar radiation is captured by PV panels and converted into heat. When the temperature rises, as the band gap of the electron conduction band movement decreases, the thermal movement of the electrons inside the semiconductor increases, thereby further increasing the saturation current. (Mertens, 2019) As the Shockley Equation stated in 2.2.1 below, increasing the saturation current will decrease the open-circuit voltage if the other variable is fixed. (Mertens, 2019)

$$V_{OC} = mV_T \ln\left(\frac{I_{SC}}{I_s}\right) \quad (2.1.1)$$

Where:

V_{OC} = Open circuit Voltage of a PV Cell, V

V_T = Terminal Voltage of a photodiode, V

I_{SC} = Short Circuit current of a PV Cell, A

I_s = Saturation of a photodiode, A

m = idealistic factor, usually in between 1 or 2

This further proved by (Amelia et al., 2016) by using PVsyst software and one piece of solar panel experiment outdoors. Figure 2.1.1 and 2.1.2 shows the PVsyst simulation result in the form of I-V and P-V curve under Standard Test Condition (STC) of 25 °C, solar irradiance of 1000 W/m², and Air mass of 1.5.

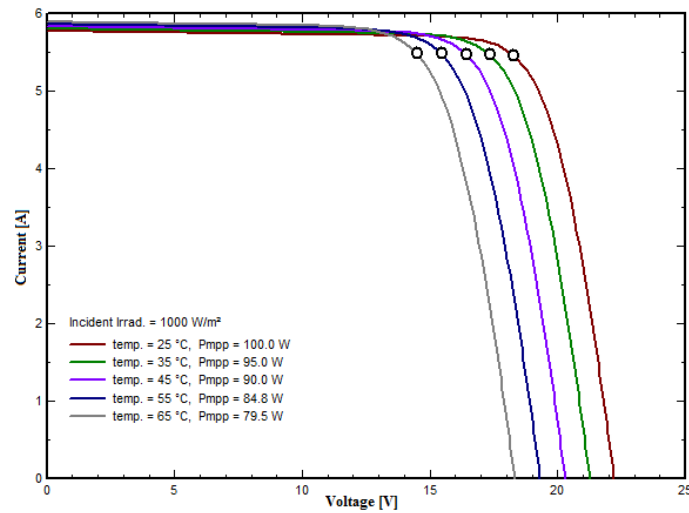


Figure 2.1.1: Current-Voltage (I-V) Curve. (Amelia et al., 2016)

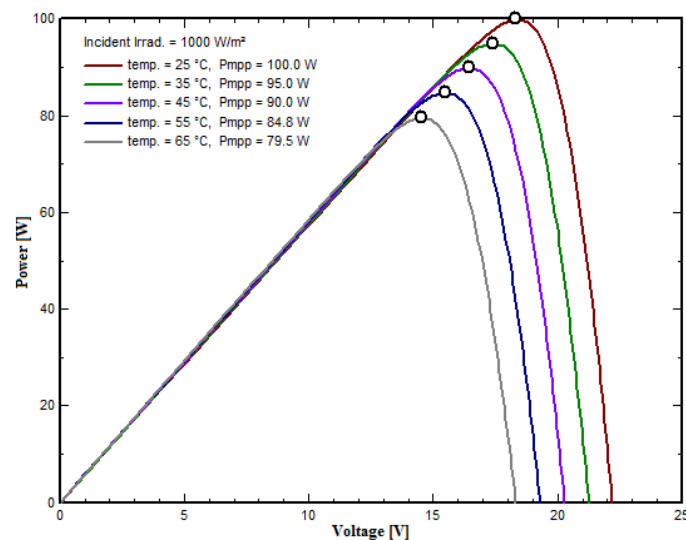


Figure 2.1.2: Power-Voltage (P-V) Curve. (Amelia et al., 2016)

These figures also show that as the temperature rises to 10 °C, the power drops to about 5 % or 5 W. In addition, when the operating temperature is 65 °C, the lowest output power of PV panel is 75 W, and at 25 °C, the highest output power of the PV panel is 100 W. (Amelia et al., 2016). It is also noticeable that the open circuit voltage of the PV panel decrease and the short circuit current of the PV panel slightly increases. (Amelia et al., 2016)

According to the experiment conducted by Indian researchers (Dash and Gupta, 2015), they found that different solar cell technologies will have a different temperature coefficient of power by increase temperature surrounding the solar panel in the environment chamber. Though the use of solar simulator

equipment, the solar irradiance is also kept constant. (Dash and Gupta, 2015)
Table 2.1.1 below showed their findings on Multi-Silicon Technologies.

Table 2.1.1: Measured Temperature coefficient for Multi C-Si technologies.
(Dash and Gupta, 2015)

Type of PV module	Module peak output (Wp)	Temperature coefficient (%/°C)			Average temperature coefficient of power (%/°C)
		Current	Voltage	Power	
Multi C-Si	75	0.031	-0.267	-0.356	-0.387
	75	0.059	-0.369	-0.506	
	12	0.036	-0.291	-0.373	
	50	0.046	-0.264	-0.346	
	50	0.033	-0.291	-0.396	
	300	0.054	-0.306	-0.428	
	75	0.001	-0.058	-0.329	
	75	0.002	-0.075	-0.364	

From the Table 2.1.1 above, they found that the average temperature coefficient of power of polycrystalline silicon PV cells were ranging from -0.329 % to -0.506 % and the average of it was -0.387 %. (Dash and Gupta, 2015)
The temperature average coefficient will be used to two equations 2.1.2 and 2.1.3 below:

$$V_{OC2} = V_{OC1}(1 + \beta(T_2 - T_1)) \quad (2.1.2)$$

Where:

V_{OC2} = Open Circuit Voltage at T_2 , V

V_{OC1} = Open Circuit Voltage at Standard Test Condition (STC), V

β = Temperature coefficient of Voltage., percentage /°C

T_2 = Operating Temperature, °C

T_1 = Temperature in STC, which was 25 °C

$$P_{OC2} = P_{OC1}(1 + \gamma(T_2 - T_1)) \quad (2.1.3)$$

Where:

P_{OC2} = Power Output at T_2 , W

P_{OC1} = Power Output at STC, W

γ = Temperature coefficient of Power, %/°C

T_2 = Operating Temperature, °C

T_1 = Temperature in STC, which was 25 °C

There are many reasons that affecting the operating temperature of PV modules. These factors include roofing material, ventilation, modular frame, and local environmental conditions. (Ye et al., 2013) Some researchers have proposed various model for these factors. The simplest model is the Ross model. Ross model is defined as the equation for the operating temperature of a PV module link with the ambient temperature and the incident solar irradiance which exclude wind and electrical load. (Skoplaki and Palyvos, 2009) The Ross model equation is shown in the 2.1.4 below. (Skoplaki and Palyvos, 2009; Ross, 1976):

$$T_M = T_A + kG_M \quad (2.1.4)$$

Where:

T_M = Module Temperature, °C

T_A = Ambient Temperature, °C

k = Ross coefficient that determine the slope between the temperature and irradiance level, °C m²/W (Ross, 1976)

G_M = Irradiance on PV module, W/ m²

An experiment that has been done by (Ye et al., 2013) is noteworthy that they found out that the average Ross coefficient, k in the tropical region such as Singapore ($k = 0.024$ °C m²/W) is higher than Europe such as Spain ($k = 0.016$ °C m²/W) and Germany ($k = 0.014$ °C m²/W) in the Figure 2.1.3 below resulting in slope is steeper.

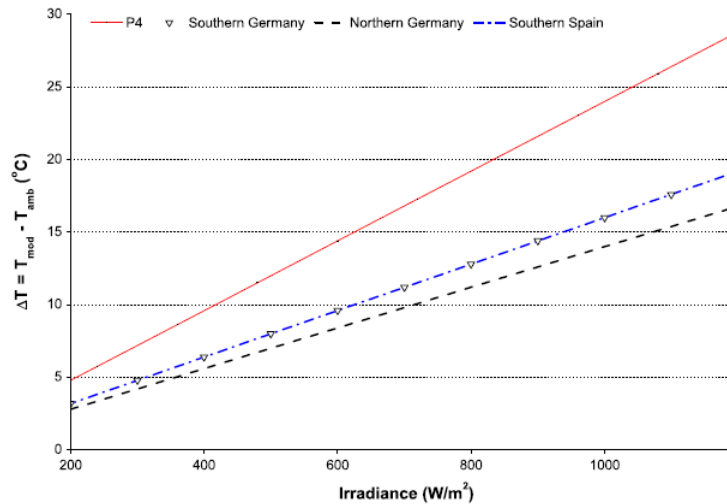


Figure 2.1.3: Graph of PV Temperature Difference between Ambient and Module Temperature versus Irradiance Comparison between Singapore (P4), Germany, and Spain. (Ye et al., 2013)

Besides that, (Ye et al., 2013) is highly recommendable for providing the information that the concrete roof has a lower k value than the metal roof unless covered by dark-coloured roof sealant, which acts as a heat absorber. It is because metal tends to absorb heat and it has low specific heating capacity.

Moreover, by increasing the distance between PV panel and rooftop, the k value will decrease due to as the distance increases, the airflow through PV panel increases, therefore the PV panel operating temperature decreases as the air carries heat out of the PV panel. It is recommended to remove any obstacles that prevent the natural air flow from entering the PV panel to further reduce the k value. (Ye et al., 2013) The evidence will further be discussed to subsection 2.2.

Next, the k value of frameless PV panel is often lower than that of aluminium frame PV panels. This fact is because the aluminium-framed PV panel tends to absorb heat also has the tendency to let the airflow slower. (Ye et al., 2013)

Finally, the k value for locations close to water or jungle areas is lower than k value found on the upper floors of the building. This fact is because the large presence of plants and water tended to decrease the operating temperature of the PV panel by cooling down on the natural surroundings. (Ye et al., 2013)

2.2 Past Research of Effect or Optimization for Ventilation on BAPV System

Therefore, it is necessary to ventilate the BAPV system, as this will reduce the operating temperature of the PV panels in the BAPV system. One way to reduce the operating temperature of PV panels is to increase the distance between PV panels and the roof or façade so that the winds flow naturally to the PV system. (Ye et al., 2013).

Around the world or in Malaysia itself, there are many researchers who tend to make valuable contributions to determine the effects and finds the best ventilation configuration between the PV panel and the roof, which will be explained in the following subsections:

2.2.1 Optimization of Air Gap for Ventilation on BAPV System by Simulation

(Gan, 2009a; b) provided an innovative way of using Computational Fluid Dynamics (CFD) FLUENT software simulation to find the critical air gap between the PV panel and roof to prevent the PV panel from overheating. The simulation is using a realistic PV module (Type B485) and performed under bright sunshine ($G_M = 1000 \text{ W/m}^2$) and no wind effect conditions where overheating of PV panels occurs. (Gan, 2009a) The roof was considered flat. The definition of the air gap is shown in Figure 2.2.1.1.

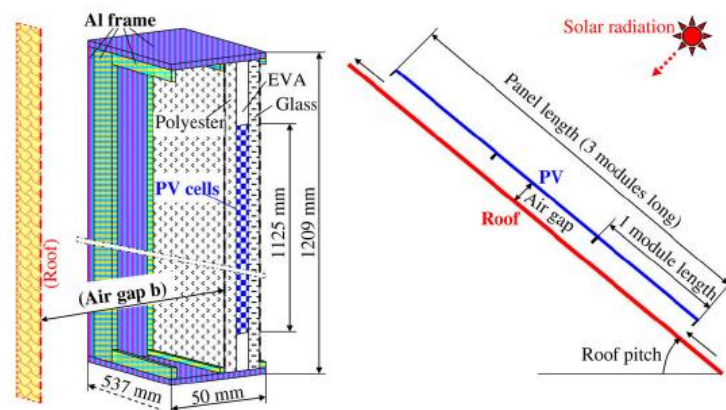


Figure 2.2.1.1: Measurement of realistic PV Module (Type B485) with Air Gap Definition in CFD Simulation. (Gan, 2009b)

Many results obtained from the simulation, including of roof pitch, the number of modules of up to three modules, and the air gap between PV and roof top, and solar irradiance. The example focused on one panel, and the change in solar irradiance based on the global solar irradiance in London on June 21 along with various roof pitches is shown in Figure 2.2.1.2. (Gan, 2009b; a)

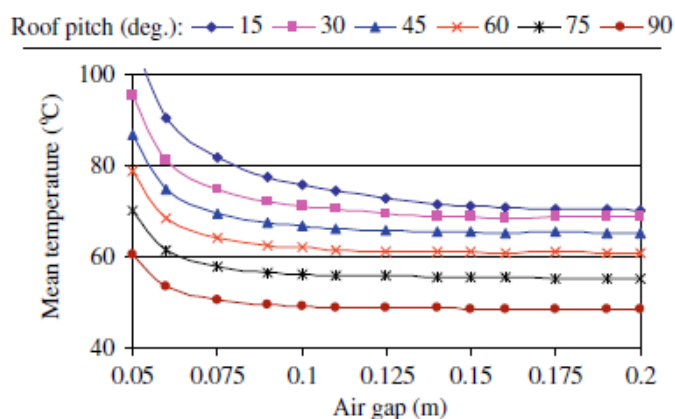


Figure 2.2.1.2: Graph of mean temperature versus air gap with various roof pitch and solar irradiance for one solar panel from the result of CFD Simulation. (Gan, 2009b)

From Figure 2.3.2 above, when the air gap increases, the mean temperature decreases regardless of the roof pitch. The result further determined by either using the graphical method or using numerical methods, but the graphical methods have a higher air gap approximation. (Gan, 2009a) Therefore, (Gan, 2009a) concluded and suggested that for the installation of a single PV panel, the air gap should be between 14 cm to 16 cm as a critical air gap for decreasing the operating temperature. It also applies to PV modules installed on the roof less than 30 degrees regarding the panel's length. (Gan, 2009a)

However, the discovery of (Gan, 2009a; b) is limited to the usage of longer and continuous solar irradiance input in European countries (such as the United Kingdom and Germany), rather than shorter and various irradiance in Malaysia. In addition, the wind speed was not considered in the study, so the operating temperature of PV panel is too high, which is unreasonable, especially on the lower roof slope in his simulation.

2.2.2 Effect of Air Gap and Type of Roof on Temperature at BAPV system based on Malaysia Climate

(Zakaria et al., 2013) discovered the key factors affecting the BAPV photovoltaic array and provided valuable contributions. They used a metal deck and eight PV modules (four monocrystalline silicon technologies and four polycrystalline silicon technologies), as well as a metal roof and a concrete roof to replicate the BAPV system. Figure 2.2.2.1 shows an example of mock-up experiments on the metal roof of the Shah Alam campus in Selangor. (Zakaria et al., 2013)



Figure 2.2.2.1: Metal-Deck roof Mock-Up Experiment on campus in Shah Alam, Selangor. (Zakaria et al., 2013)

(Zakaria et al., 2013) measured the PV panels operating temperature by using K-type thermocouples, irradiance by using Kipp & Zonen SP LITE 2 pyranometer and logged using the DataTaker data logger. The data obtained for two consecutive days. Table 2.2.2.1 shown on the result of temperature difference at PV panels operating temperature and ambient temperature when using poly silicon-technologies at the metal roof varies with air gap and solar irradiance. (Zakaria et al., 2013)

Table 2.2.2.1: Table of Irradiance, Height and Temperature Difference between 4 Type of Configuration. (Zakaria et al., 2013)

Irradiance / Wm ²	Height/ cm	Temperature Difference / ΔT / °C			
		Mono- Concrete	Mono- Metal	Poly- Concrete	Poly- Metal
300	0	15.7	6.9	11.7	2.5
	10	13.2	8.2	6.7	8.6
	20	8.4	6.2	5.9	3.8
500	0	19.0	7.0	14.2	15.8
	10	15.6	11.2	10.8	13.5
	20	10.3	9.8	9.5	4.3
800	0	25.1	12.9	20.8	24.0
	10	19.8	17.5	18.9	15.3
	20	14.5	17.1	13.9	13.9

Based on the Table 2.2.2.1 above, (Zakaria et al., 2013) had found out and concluded that factors affecting PV temperature are roof material, air gap, type of PV modules and solar irradiance levels. First, the concrete roof has a higher temperature difference than the metal roof had found out. Next, poly-Si has a higher temperature difference than mono-Si in the metal roof but has a lower temperature in the concrete roof. The temperature difference will decrease as the air gap increase and increases as solar irradiance increases. (Zakaria et al., 2013)

(Zakaria et al., 2013) also found out the relationship between cell temperatures, ambient temperature during morning 7:00 a.m., and 1:00 p.m. is increasing. Figure 2.2.2.2 shows and proves the above statement by drawing a graph of the operating temperature of the polysilicon PV panel on the metal roof, versus the ambient temperature along with the difference of air gap:

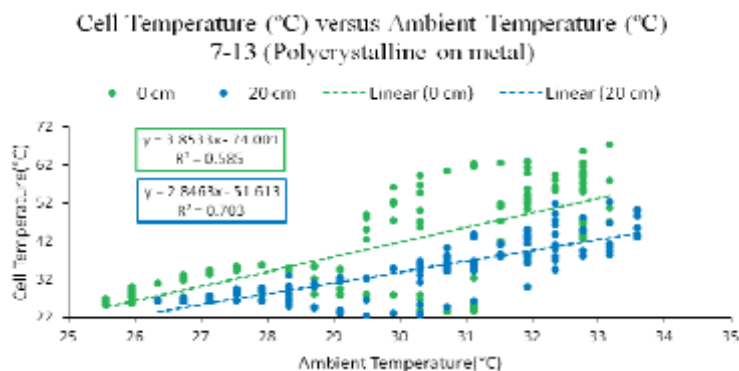


Figure 2.2.2.2: Graph of Cell Temperature versus Ambient Temperature with Poly-Si, metal deck at different air gaps. (Zakaria et al., 2013)

In conclusion, (Zakaria et al., 2013) concluded that as the air gap increases, Ross coefficient k will decrease. Besides that, the finding is classification together with the International Energy Agency (IEA) classification where 0 cm and 10 cm categorized as not so well cooled and 20 cm as well cooled. Hence, 20 cm can be considered as the optimal gap. (Zakaria et al., 2013)

However, (Zakaria et al., 2013) explanation is not plausible since questions arise about how to find out the Ross coefficient from the graph of cell Temperature versus Ambient temperature as stated in equation 2.1.4. Besides that, wind speed did not consider in this experiment. Moreover, the result in Table 2.2.2.1 is not consistent with the conclusion said as the air gap increases, the temperature difference between ambient temperatures and cell temperature is decreasing since taken only one result. Finally, yet importantly, the power generated by the PV is not taken during the entire project. (Zakaria et al., 2013)

Therefore, (Ho, 2015; Chong, 2015; Chew, 2015) provides an innovative way for improving (Zakaria et al., 2013) research methods of key factors affecting the performance of the BAPV system in Malaysia.

2.2.3 Effect of Inclination Angle and Type of Roof on Temperature at BAPV system based on Malaysia Climate

(Ho, 2015) provided a valuable contribution by replicating retrofitted installation by using the metal deck and 3 same multi-Si technology's PV modules with concrete roof and reflective coated zinc roof to studying the effect of roof type and tilting angle on the temperature of PV and the performance of

PV systems. Figure 2.2.3.1 showed his mock-up experiment in Bandar Sungai Long, Selangor. (Ho, 2015)



Figure 2.2.3.1: Metal-Deck Roof Mock-Up Experiment in Bandar Sg Long, Selangor. (Ho, 2015)

Similar for (Zakaria et al., 2013), (Ho, 2015) measured the PV module temperature by using Maxim/Dallas DS18B20 temperature sensor, ambient temperature by using DHT 22 temperature sensor, solar irradiance by using pyranometer or solar meter, voltage and current by using a Multimeter, wind speed by an anemometer. (Ho, 2015)

Besides that, (Ho, 2015) also fixed the air gap between the concrete roof and PV panel as 3 cm, and the air gap for metal deck and PV panel as 8 cm. The slanting angle for his experiment was varied with 0° , 9° , and 18° . PV module and ambient temperature data recorded by using Arduino Mega 2560 and with Adafruit Data Logger Shield, while other parameters (such as solar irradiance and wind speed) were acquired in a limited time. These results of these various configurations of the experiment taken by these devices on two consecutive days. A large numbers of result have been obtained .Table 2.2.3.1 gives a summary of PV module temperature versus the solar irradiance in different roof materials and tilt angles in a linear equation. (Ho, 2015)

Table 2.2.3.1: Summary of correlation on PV Cell Temperature versus Solar Irradiance in Different Roof Materials and Inclination angle. (Ho, 2015)

PV Cell Temperature Versus Solar Irradiance	0°	9°	18°
Metal Roof	$y=0.0185x+53.273$ $R^2 = 0.3504$	$y = 0.0134x+ 54.56$ $R^2 = 0.3567$	$y=0.0215x+43.962$ $R^2 = 0.6481$
Concrete Tile	$y=0.0137x+52.126$ $R^2 = 0.3193$	$y=0.0103x+53.007$ $R^2 = 0.2828$	$y=0.0187x+43.248$ $R^2 = 0.6519$
Control	$y=0.0168x+46.781$ $R^2 = 0.4174$	$y=0.0115x+48.446$ $R^2 = 0.4039$	$y=0.0186x+39.674$ $R^2 = 0.6879$

According on Table 2.2.2.2 above, (Ho, 2015) had noticed that even if the air gap of the concrete roof is smaller than that of the metal deck, the Ross coefficient on a metal roof is higher than that of the concrete tile roof. In addition, (Ho, 2015) found out that when the tilt angle is increase, the Ross coefficient decreases from 0° to 9°, and then increased from 9° to 18°.

Moreover, (Ho, 2015) analysed the relationship between power loss and solar irradiance and found that when the tilt angle increase, the power loss of solar panel panels will decrease. Table 2.2.3.2 shows a summary of the correlation based on the relationship between power loss and solar irradiance. According to the following Table 2.2.3.2, he also noticed that although the air gap of the metal roof is larger than that of the concrete roof, the power loss of the metal roof will be greater than that of concrete roof.

Table 2.2.3.2: Summary of correlation on Power Loss versus Solar Irradiance in Different Roof Materials and Inclination angle. (Ho, 2015)

Power Loss Versus Solar Irradiance	0°	9°	18°
Metal Roof	$y=1e-04x + 0.0979$ $R^2 = 0.4965$	$y=6e-05x + 0.1216$ $R^2 = 0.3567$	$y= 9E-05x +0.078$ $R2 = 0.6481$

Concrete Tile	$y = 8e-05x + 0.0937$ $R^2 = 0.5091$	$y = 4e-05x + 0.1152$ $R^2 = 0.2828$	$y = 8E-05x + 0.075$ $R^2 = 0.6519$
Control	$y = 8e-05x + 0.0786$ $R^2 = 0.5498$	$y = 5e-05x + 0.0964$ $R^2 = 0.4039$	$y = 8e-05x + 0.0603$ $R^2 = 0.6879$

In short, (Ho, 2015) concluded that when solar irradiance increases, the difference between ambient and PV panel operating temperature is increased further increase, resulting in a decrease in output voltage, which will eventually increase the power loss on the PV system. In addition, (Ho, 2015) pointed out that when the tilt angle increase, the natural ventilation effects will be better, which will reduce in the operating temperature of the PV panel.

However, (Ho, 2015) research location is underestimated the shading effect of the building and surrounding on the PV system which will cause further decline in the efficiency of the PV panels. Besides that, the solar irradiance taken is limited by time, so that the graphical result of solar irradiance between 400 W/m² to 800 W/m² is less. Moreover, the air gap between the concrete roof or the metal roof and the metal deck is not consistent.

2.2.4 Effect of Inclination Angle and Air Gap on Temperature of BAPV system based on Malaysia Climate

(Chew, 2015) has made a significant contribution in providing the influence of the tilt angle and air gap on the operating temperature of the BAPV system. The experimental setup is similar to (Ho, 2015), but all experiment use metal roofs. Figure 2.2.4.1 shows his mock-up experiment in a similar location. (Ho, 2015).



Figure 2.2.4.1: Metal-Deck Roof Mock-Up Experiment in Bandar Sg Long, Selangor. (Chew, 2015)

Similar for (Zakaria et al., 2013; Ho, 2015), (Chew, 2015) measured the PV module temperature by using LM35 temperature sensors, ambient temperature by using DHT 22 temperature sensors, irradiance by using a solar meter, voltage, and current by using Multimeter and wind speed by an anemometer. (Chew, 2015)

Besides that, (Chew, 2015) changed the air gap between the metal deck and PV panel from 0 cm to 20cm. The slanting angle for his experiment was varied with 0° , 10° , and 20° . PV module and ambient temperature data recorded by using Arduino Mega 2560 and Adafruit data logger shield. Plenty of results had taken and Figure 2.2.3.2 shows the graph of operating temperature on the PV system versus the solar irradiance in various air gap distances and no slanting angle. (Chew, 2015)

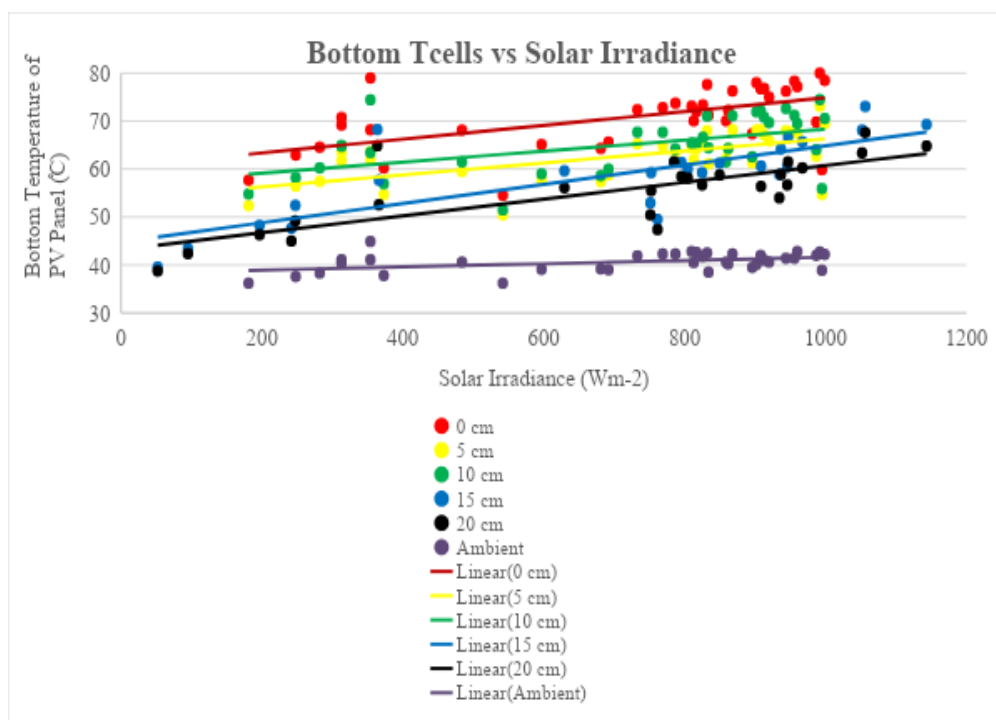


Figure 2.2.4.2: Graph of PV Operating Temperature versus Solar Irradiance at various Air Gap with Zero slanting angle. (Chew, 2015)

Figure 2.2.4.2 above shows that the temperature of the PV panel is decreasing when the air gap from the PV panel and the roof deck is increasing. Hence, the graph of the PV operating temperature versus the solar irradiance showed a shift down. (Chew, 2015)

In conclusion, (Chew, 2015) concluded that the efficiency of the PV panel can be increased by up to 1.32% when the tilt angle is 20° and the gap is 20 cm compared with no air gap and tilt angle is 0° . When the tilt angle is increased, the influence of natural convection increase, and when low solar radiation occurs, the influence of the air gap occurs..

However, similar to (Ho, 2015), (Chew, 2015) research location underestimated the shading effect of the building and surrounding environment on the PV system which will cause further reduce in the efficiency of PV panels. Besides that, the Ross coefficient values of the entire experiment has not been determined. Moreover, some of the results of the experiment in slanting angle 10° and 20° were not valid because it is not possible that when there was an increment in the solar irradiance, there was a decrement in cell temperature in same air gap condition.

2.2.5 Effect of Forced Convection on Temperature of BAPV system based on Malaysia Climate

(Chong, 2015) provided an innovative way by adding fans below PV panel below to replicate retrofitted installation by using the metal deck and 3 same poly-Si technology PV modules with reflective coated zinc roof similar to (Chew, 2015) for studying the effect of forced convection onto temperature of BAPV system. Figure 2.2.5.1 shows his BAPV system configuration for forced convection experiments.

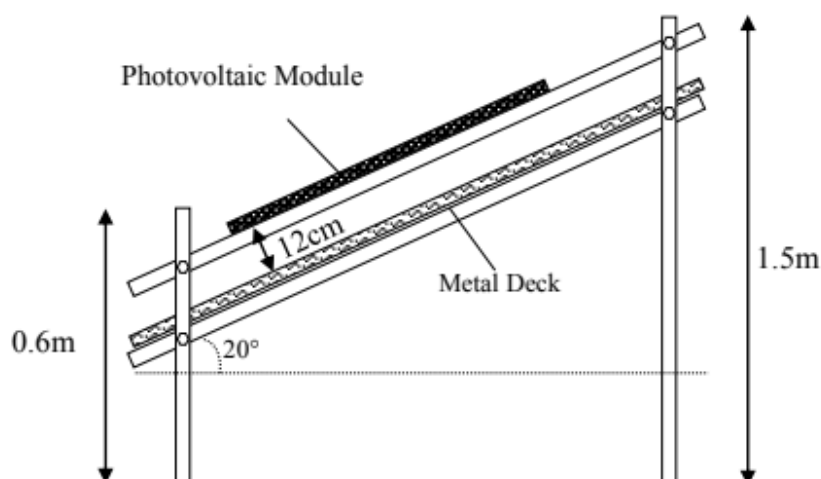


Figure 2.2.5.1: BAPV system configuration setting with Air Gap and slanting angle definition. (Chong, 2015)

Similar for (Zakaria et al., 2013; Ho, 2015; Chew, 2015), (Chong, 2015) measured the PV module temperature by using DS18B20 temperature sensors, ambient temperature by using DHT 22 temperature sensor, irradiance by using pyranometer, voltage and current by using multi-meter and wind speed by an anemometer. In addition, (Chong, 2015) uses 4 Deep Cool XFAN 120L axial fan to place under the PV system to demonstrate forced convection to the BAPV system. Figure 2.2.5.2 shows the actual position of fan, and Table 2.2.5.1 shows the summary configuration of the fan on the BAPV System.



Figure 2.2.5.2: Fan System beneath the BAPV system. (Chong, 2015)

Table 2.2.5.1: Summary of experimental fan configuration in the BAPV system. (Chong, 2015)

Experimental No.	PV system 1	PV System 2	PV System 3
1	4 Fan Put Beneath Bottom of system	4 Fan Put Beneath Top of the system	No fan attached at bottom of PV System
2	4 Fan Put Beneath Bottom of system Additional of Wind Block	4 Fan Put Beneath Top of system Additional of Wind Block	
3	4 Fan Put Beneath Bottom of system	4 Fan Put Beneath Bottom of system Additional of Wind Block	

4	8 Fan Put Beneath Bottom and Top of system Additional of Wind Block	4 Fan Put Beneath Bottom of system	
5	4 Fan Put Beneath Bottom and Top of system Additional of Wind Block	2 Fan Put Beneath Bottom of system	
6	4 Fan Put Beneath Bottom of the system with a slanting angle of 90°	4 Fan Put Beneath Bottom of the system with a slanting angle of 75°	

. Plenty of results had taken by (Chong, 2015) and he found out that when the axial fan installed at the bottom part of the PV Panel, the operating temperature of PV decreased the most comparing with reference and fan, which installed on top for extracting the heat inside PV system. Besides that, the wind block will block the natural wind will cause the operating temperature increase compared with no wind block had found. Moreover, axial fans installing the bottom and top of the PV system with the wind block will be having better performance than axial fans installing only the bottom of the system had found out.

In conclusion, (Chong, 2015) concluded that installing an axial fan at either bottom of the PV System for blowing or top of the PV system for extracting with a slanting of 90° will having a more operating temperature of PV system drop compared with natural convection on a PV system. In addition, the fact that the power increase of the PV system cannot compensate for the power consumption of the axial fan had been found.

However, similar to (Ho, 2015; Chew, 2015), (Chong, 2015) research location has been underestimated the shading effect of the building and surrounding on the PV system which will cause further PV panel efficiency drop. Besides that, the solar irradiance taken was limited by time so that the result of

solar irradiance lesser. Moreover, the Ross coefficient is not determined due to the graph of irradiance and average temperature not plotted.

2.3 Summary

To conduct more exact experiments, various journals, thesis, and article were reviewed. In short, excepting the air gap between PV panels and roof top, other factors, which are affecting the PV operating temperature stated by (Ye et al., 2013; Gan, 2009b; a; Zakaria et al., 2013; Ho, 2015; Chew, 2015) must be the same condition or removed. Hence, the BAPV system should be experimented in open areas. One example is the roof top of the tallest building to avoid shading the PV panel. Besides that, the experiment should be performed under the same roof material and the same roof tilt angle. In addition, the experiment should be performed on the same type of PV panels.

CHAPTER 3

METHODOLOGY AND WORK PLAN

3.1 Experimental Setup

The main objective of the study is to analyse, model and optimize the air gap distance between solar PV panel and the metal deck on the performance of PV panel by determining the operating temperature and electricity generation output of the PV panel.

First, the location of the research is set in UTAR KB block rooftop to reduce the shading effect also maximise the solar irradiance effect on the experimental PV panel to meet the recommendations stated in literature review. Besides that, there is a weather station near the location to obtain valuable variables such as solar irradiance and wind speed. Figure 3.1.1 below shows the block diagram setup in this study.

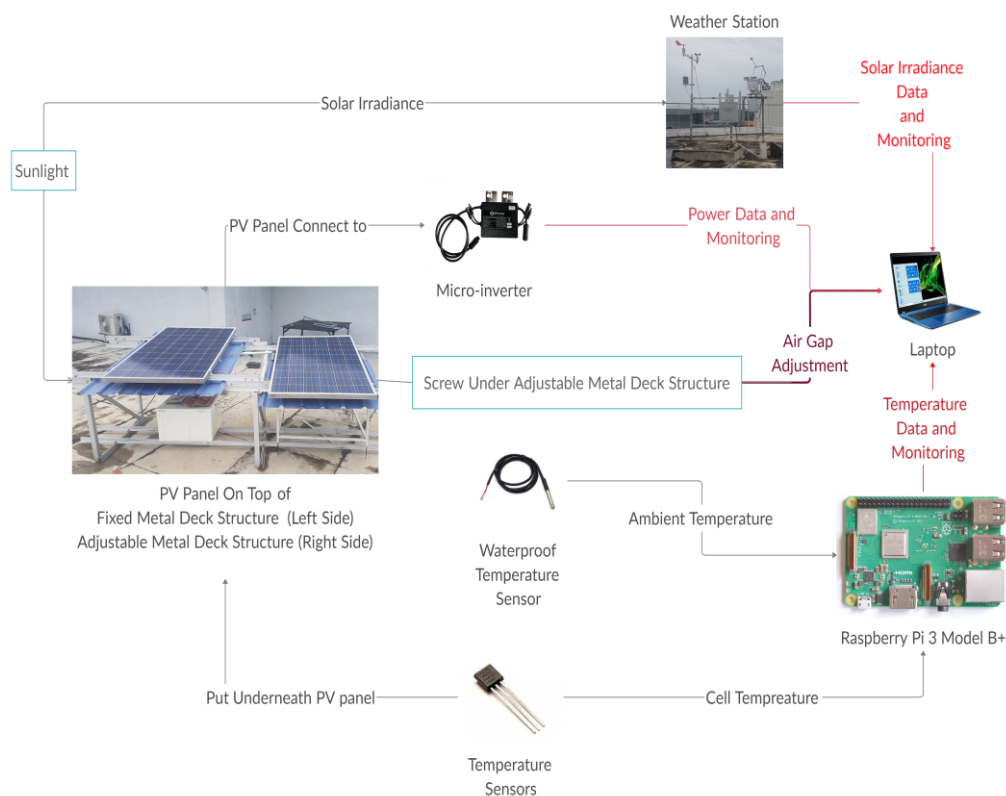


Figure 3.1.1: Experimental Setup Block Diagram for determining the effect of the air gap for ventilation of BAPV systems.

As shown in the block diagram shown in Figure 3.3.1 above, two PV panels are placed on top of the fixed metal deck structure and the adjustable metal deck structure. The four screws under adjustable metal deck structure can be adjusted to change the air gap distance. The structure is placed to expose to sunlight, and the solar irradiance on the PV panels are recorded in the weather station.

Eight temperature sensors are placed on the both PV panels back sheet to read operating temperature of PV panel. While the water-proof temperature sensor is placed around the metal deck structure and reads the ambient temperature. These temperature data are recorded in the Raspberry PI data logger in Microsoft Excel Comma Separated Values (CSV) files.

Both PV panels are connected to a micro-inverter to obtain the power output of PV panels. Then obtain and monitor these the previously described data from the laptop. Figure 3.1.2 below shows the actual set up diagram based on the block diagram in Figure 3.1.1.

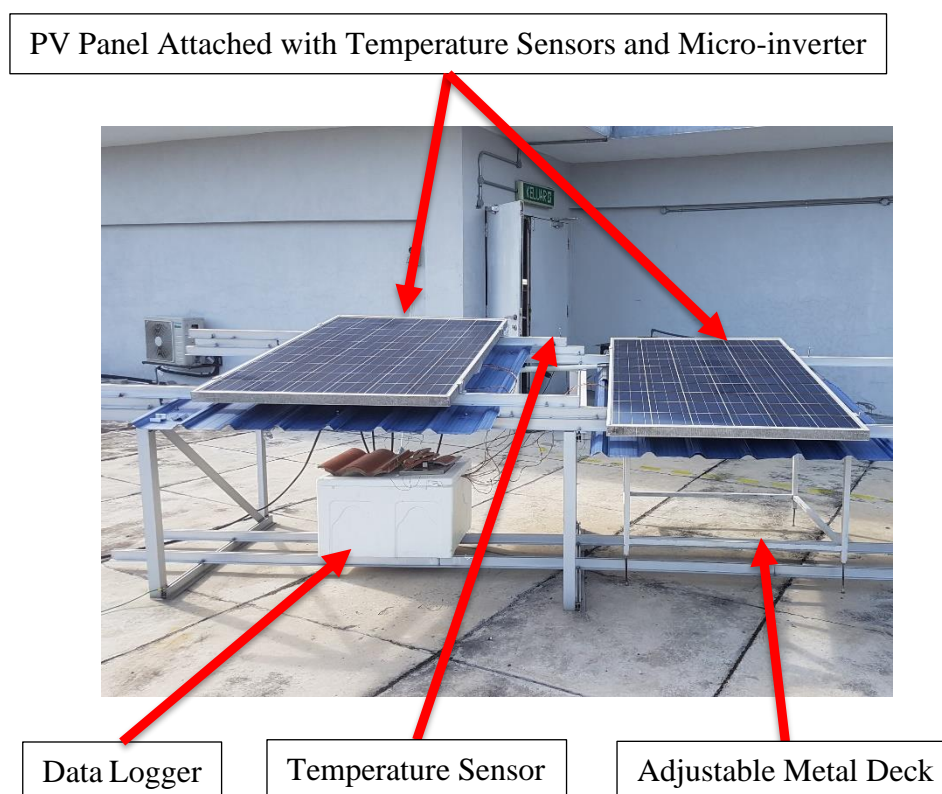


Figure 3.1.2: Actual Setup Diagram to determine the effect of the air gap for ventilation of BAPV systems.

After determining the research site and briefing the block diagram procedures. The details of installation of the metal deck model and PV System and will be further discuss in Section 3.3.1.

3.1.1 Metal Deck and PV System Setup

First, the metal deck and the model of the rooftop and its measurement provided need to be determined and constructed. As shown in Figure 3.1.1.1 below, the metal deck installed under the aluminium supporting structure provided by UTAR facility with a measurement of 75 cm- 95 cm *111 cm * 364 cm. The adjustable metal desk measures as 63 cm- 81 cm*100 cm*100 cm. Besides that, it provided with an adjustable threaded rod up to 12 cm. This measurement was performed for making sure the inclination angle to be fixed at 10°. To proving the measurement is correct, trigonometry such as the tangent rule has used as the equation 3.1.1.1 below.

$$\tan \theta = \frac{\text{Opposite of a Traingle}}{\text{Adjecnt of a Traingle}} \quad (3.1.1.1)$$

After using equation 3.1.1 above, the tilting angle for supporting frame and metal desk is 10.21° and 10.20° respectively.

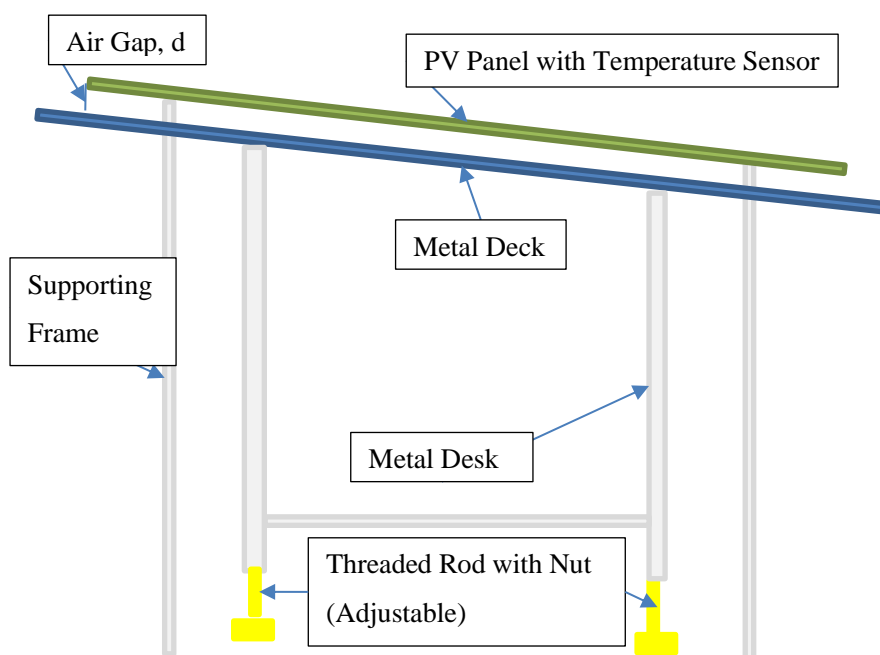


Figure 3.1.1.1: Sketching of Installation of Metal Deck.

After installing the metal deck, install the PV panel on the support frame. However, before installing the PV system on the support frame, the temperature sensors needs to be installed on the back of the PV Panel using thermal paste and aluminium foil tape. The PV panel must put on the micro-inverter to measure the power output. Each of the PV panel install with one port of the AP System YC500A micro-inverter for power measurement and four DS18B20 temperature sensors installed at the rear surface with the orientation as the Figure 3.1.1.2 below for measuring the operating temperature of PV Panels. The measured temperature will be sent to the Raspberry PI for data storage, and the data recording method will discuss in Section 3.1.2.

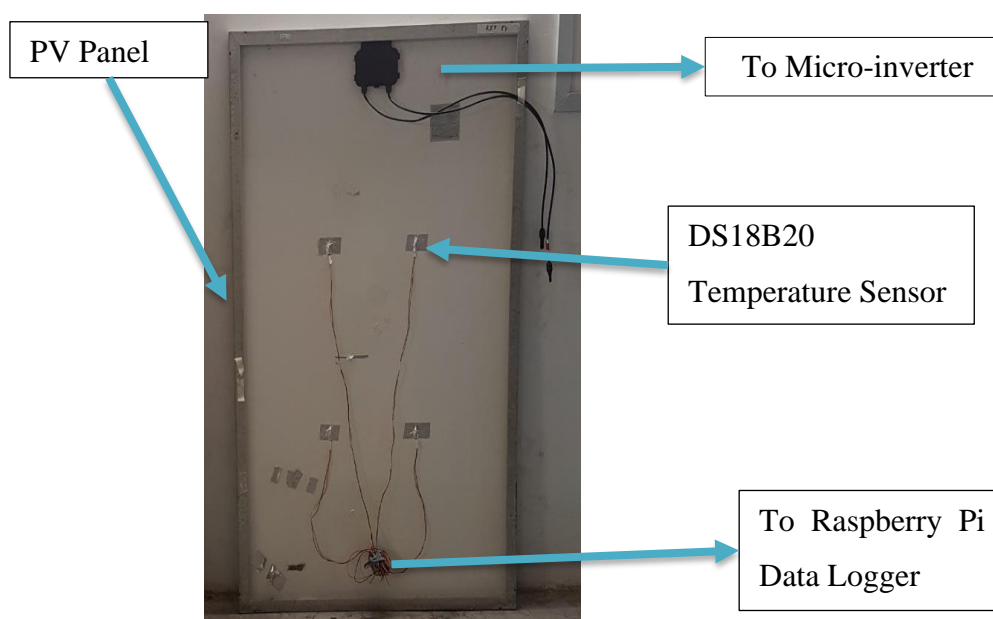


Figure 3.1.1.2: Installation of Components on PV Panel.

3.1.2 Raspberry PI 3 Temperature Data Logger

Figure 3.1.2.1 briefly introduces the structure of the Raspberry Pi 3 temperature data logger. Eight DS18B20 temperature sensor transistors read the operating temperature of the PV Panel, and one DS18B20 temperature sensor waterproof module reads the ambient temperature around the BAPV system. These two kinds of temperature data are recorded every 30 seconds, and the readings are stored in the CSV file along in real-time along with global time coordination +8. The data recorded is also checked from time to time by using Thing Speak or OverGrive platforms.

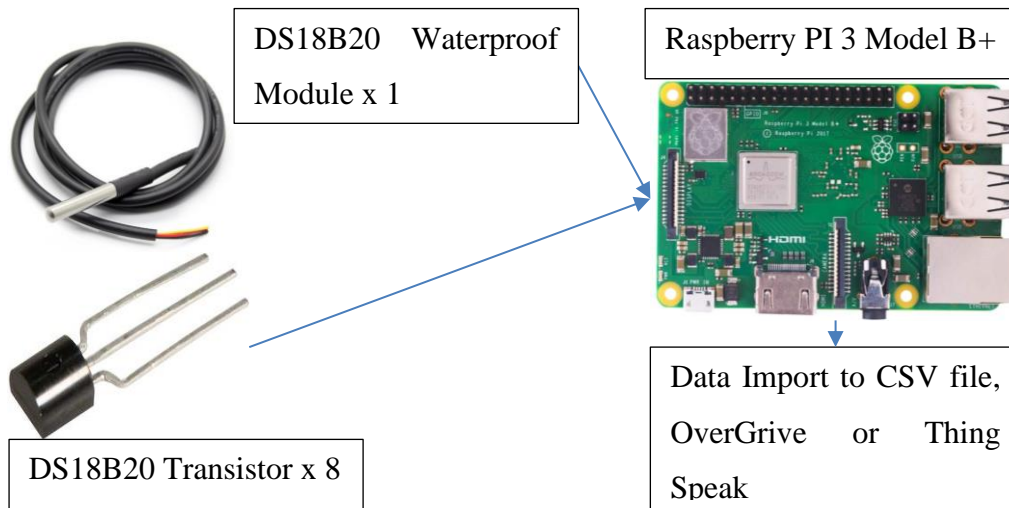


Figure 3.1.2.1: Component used for Temperature Data Logger.

Figure 3.1.2.2 shows a hardware schematic diagram of a Raspberry PI 3 Model B+ and 9 DS18B20 temperature sensors connected by using Fritzing software. The figure also shows that all the temperature sensors are connecting in parallel with a $4.7\text{ k}\Omega$ resistor. All ground pin is connecting to pin 6 of the Raspberry PI 3, while all V_{CC} pin is connecting to pin 1 of the Raspberry PI 3 and all Data pin of the temperature sensors is connecting to pin 7 of the Raspberry PI 3.

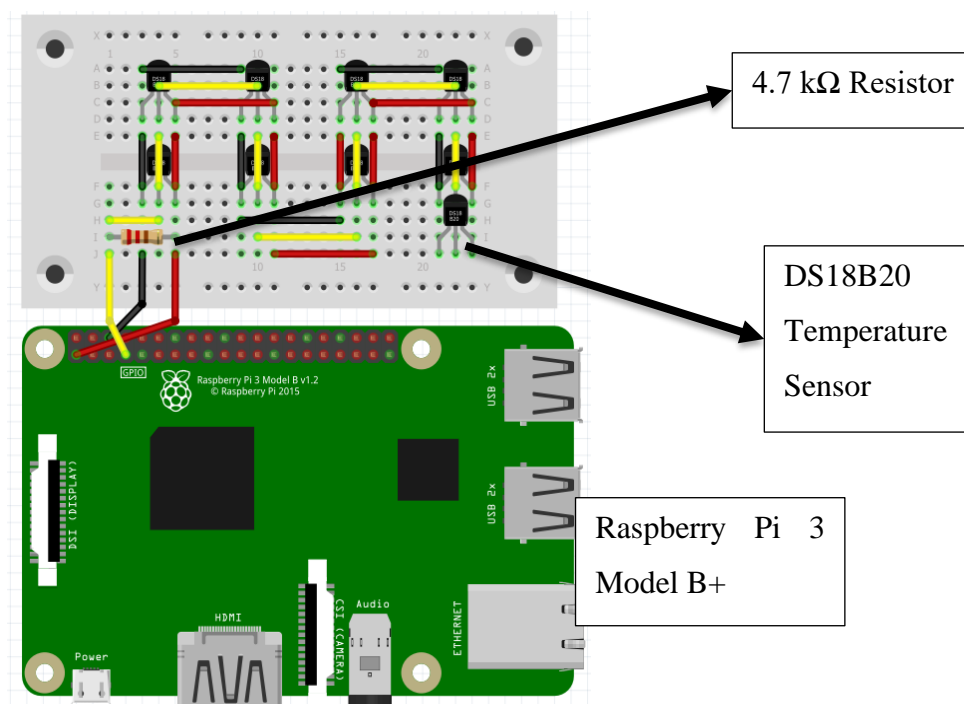


Figure 3.1.2.2: Temperature Data Logger Hardware Schematic Diagram.

The data logger is programmed by using Python language coding in Raspberry Pi 3 such a way that all temperature is recorded in Microsoft Excel CSV format with date and time in the Raspberry Pi Micro-SD Card itself also monitoring real-time by using Thing Speak or Overgrive platform. Appendix A shows the codes used to measuring the ambient temperature and operating temperature of PV panels.

After completing all the hardware connections and software programming of the data logger circuit, connect the data logger to a 5 V, 2.1 A power supply and store it in a polystyrene box to protect it from rain.

3.2 Apparatuses & Instrument

The equipment and instruments used in this research are listed below:

1. Poly-crystalline PV Panels
2. Metal Roof Deck (Fixed and Adjustable)
3. Raspberry Pi 3 Model B+
4. DS18B20 Temperature Sensors
5. 4.7k Resistor
6. Cable and Wires
7. Multimeter
8. AP System YC500 Micro-inverter

3.2.1 Poly-crystalline PV panels

In this research, two of Malaysian Solar Resources (MSR) model MYS-60P/B3/CF 260 polycrystalline PV panels were used. This panel consists of 60 solar cells. In addition, the rated maximum power STC of the PV panel is 260 W. Not only that, Open circuit voltage, V_{OC} of PV panels are 37.96 V while Short Circuit Current, I_{SC} of PV panels are 9.01 A. Moreover, the panel also having a temperature coefficient of power, γ of -0.4112 %/°C and temperature coefficient of voltage, β of -0.3137 %/°C. Figure 3.2.1.1 shows on one of the PV panels before installation on the metal deck.



Figure 3.2.1.1: Malaysian Solar Resources (MSR) model MYS-60P/B3/CF 260 polycrystalline PV panel.

3.2.2 Raspberry Pi 3 Model B +

To collect temperature data from the temperature sensor, Raspberry Pi 3 B+ is used for ambient temperature and PV panel temperature collection. Raspberry Pi 3 Model B+ is a mini desktop computer with a 1.4 GHz quad-core processor. It has a 40-pin, 27 of which are the general-purpose input-output (GPIO) pin, support full-size High Definition Multimedia Interface (HDMI), and 4 Universal Serial Bus (USB) ports. In addition, it has a Micro SD port for loading the operating system and data storage. Figure 3.2.2.1 shows the Raspberry Pi 3 Model B+.

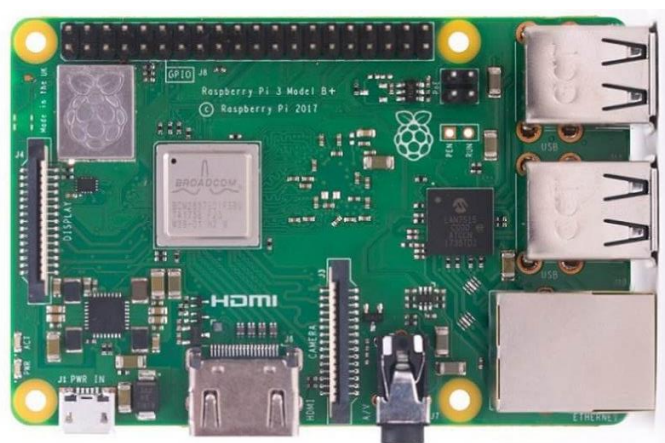


Figure 3.2.2.1: Raspberry Pi Model 3 B+

3.2.3 DS18B20 Temperature Sensors

The temperature sensor is important for this research method of measuring the ambient temperature, and the operating temperature of PV panels. Therefore, DS18B20 Temperature Sensor transistor type is used for measuring operating temperature of PV panels and waterproof module is used to measure ambient temperature. Each type of temperature sensor provides 9 to 12-bit temperature readings, which indicate the temperature of the device. Besides that, the temperature sensor powered by a 3~5 V of power supply. Not only measure temperature from -55 °C to 125 °C, but they have an accuracy range of ± 0.5 °C from -10 °C to 85 °C. Figure 3.2.3.1 shows the DS18B20 temperature sensor waterproof module and transistor type.



Figure 3.2.3.1: DS18B20 Temperature Sensor (Left: Waterproof Module, Right: Transistor Type)

3.2.4 AP System YC500 Micro-Inverter

To collect power output from PV panels over some time, AP System YC500 micro-inverter is used for the power output of PV panel collection. Like a string inverter, Micro-inverter is a type of inverter that's converts Alternating Current (AC) to Direct Current (DC) but it installed in each solar PV panel. This micro-inverter can manage 2 PV at the same time. Not only that, but it has its own independent Maximum Point Power Tracking (MPPT) on each module. Moreover, the inverter has a peak efficiency of 95.5 %. The output power will

be updated every 5 minutes to Energy Management Analysis (EMA) on the AP System's website. Figure 3.2.4.1 shows the AP System YC500 micro-inverter.



Figure 3.2.4.1: AP System YC500 micro-inverter.

3.3 Overall Project Procedure

Figure 3.3.1 shows that the entire research process. The details of the mechanical structure, Raspberry Pi data logger, and PV system layout have been discussed in Sections 3.1. However, the calibration of temperature sensors and PV panels, data collection, and data analysis will be discussed further in Sections 3.4, 3.5 and 3.6.

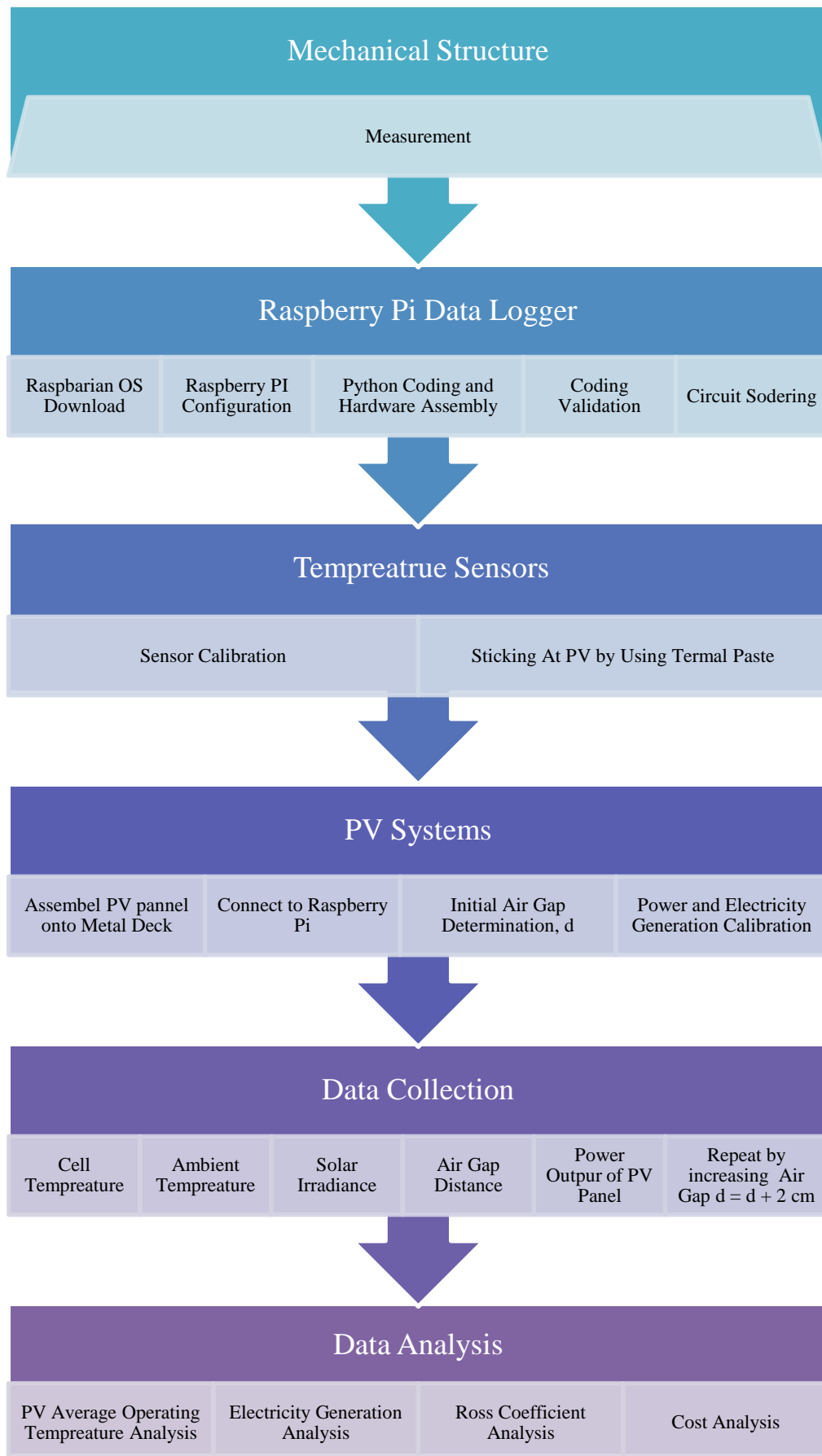


Figure 3.3.1: Overall Research Procedure

3.4 Experimental Preparation

After constructing the Raspberry Pi Data Logger circuits and its Python coding is validate, further calibration of temperature sensors and PV panel is needed to not only reduce the error on the research, but also the effect of the errors can be adjustable to the logical condition. The discussion of temperature sensor and PV calibration will be conducted in Sections 3.4.1 and 3.4.2 below.

3.4.1 Temperature Sensors Calibration

Before installing the DS18B20 temperature sensor on the back sheet of PV panels, it must be calibrated to determine the temperature difference of the sensor and other sensors or boiling water. The difference in the measurement of the temperature of the sensor will give an impact on the measurement of the operating temperature at the backside of the PV panel.

To calibrate the DS18B20 waterproof temperature sensor, the sensor should be placed in boiling water for 20 minutes. Figure 3.4.1.1 shows the DS18B20 waterproof temperature sensor is being calibrated in boiling water.



Figure 3.4.1.1: DS18B20 Waterproof Temperature Sensor Calibration by using Boling Water.

The temperature data is obtained from the Raspberry PI data logger CSV file and monitored by Think Speak IoT database. Finally, and equally important, the relative temperature difference between the temperature sensor and boiling water is determined following equation 3.4.1.1.

$$\Delta T_N = T_N - T_W \quad (3.4.1.1)$$

Where:

ΔT_N = Relative temperature difference between the sensor and boiling water, °C

T_N = Temperature recorded at the sensor, °C

T_W = Temperature of boiling water, which is equal to 100 °C

To calibrate the DS18B20 transistor temperature sensors, place eight DS18B20 transistor temperature sensors on a thin metal plate and paste them together with thermal paste and aluminium foil tape. Next, heat the metal plate to about 75 °C with boiling water, as shown in Figure 3.4.1.2 below.



Figure 3.4.1.2: Insertion of metal plate into Boiling Water for DS18B20 Temperature Sensor Calibration.

Next, take out the metal plate to cool for about 15 minutes. The data is monitored and getting by using the Think Speak IoT database. Finally, it is important that the relative temperature difference between the first temperature

sensor and other temperature sensor is determined by the following equation 3.4.1.2.

$$\Delta T_N = T_N - T_1 \quad (3.4.1.2)$$

Where:

ΔT_N = Relative temperature difference between the first sensor and next sensor, °C

T_N = Temperature recorded at the next sensor, °C

T_1 = Temperature recorded at the first sensor, °C

The relative difference between the first temperature sensor and another temperature sensor should be as small as possible. As a result, all relative differences between the tested sensor and the first sensor are in the range of ± 0.5625 °C.

After calibrating all temperature sensors, use thermal paste and aluminium foil tape to place these temperature sensors on the back of PV panels, as shown in Figure 3.4.1.3 below. Thermal paste is used because it can eliminate space in between temperature sensor and back sheet of PV panels while the aluminium foil tape is used because it is sticky, and it has high tension, so it does not lose its adhesive easily.



Figure 3.4.1.3: Attachment of DS18B20 Temperature Sensors underneath PV panels.

3.4.2 PV Panels Calibration

After installing the temperature sensors on the back sheet of the PV panel, construct structure of the PV system as in with a micro-inverter according the requirements in Section 3.3.1. After constructing the PV system, the distance between the PV panel and the roof is determined as a reference air gap. Figure 3.4.2.1 and equation 3.4.2.1 show the measurement and calculation for the purpose of initial air gap distance determination.

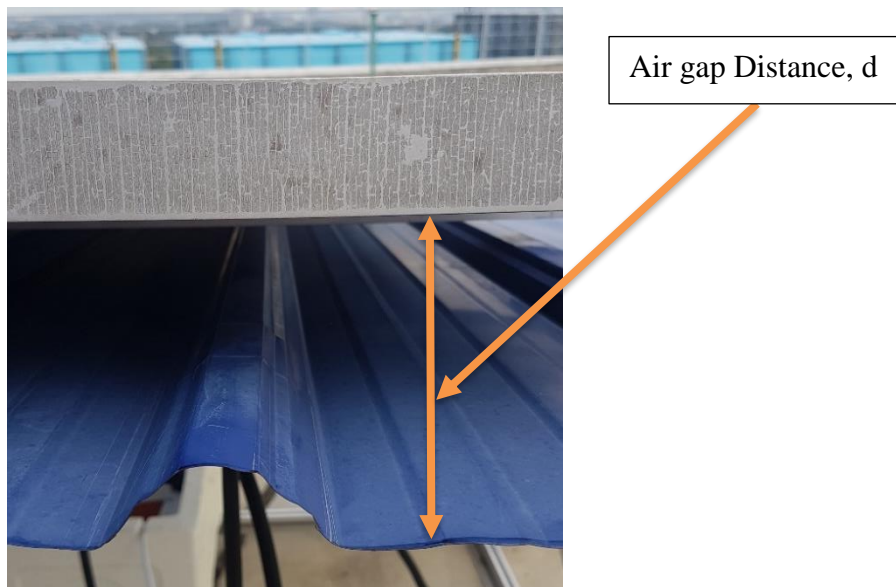


Figure 3.4.2.1: Measurement of air gap distance between the PV panel and metal deck roof.

$$d_f = d + d_{PV} - d_{Cell+EVA} \quad (3.4.2.1)$$

Where:

d_f = Final air gap distance, cm

d = Air gap distance between roof and PV panel frame as shown in Figure 3.4.2.1., cm

d_{PV} = Thickness PV panel aluminium frame, which is equal to 4.2 cm.

$d_{Cell+EVA}$ = Thickness of the solar cell and glasses in the PV panel, which is equal to 0.7 cm.

By using the above figure and equation, the initial air gap distance is determined to be 12.5 cm. After determining the air gap distance, the PV panel must be calibrated with another PV panel under same condition of rating, position, location, time, and air gap distance. First, two PV panels must be arranged side-by-side, so that the solar irradiance value on the PV panel is like the following Figure 3.4.2.2 below.



Figure 3.4.2.2: Setting of Two PV panels side by side.

The power output of two PV panels is connected to the same micro-inverter and the air gap distance between the metal deck roof and PV panel is the same. Then, the micro-inverter is automatically acquired the value of power at an interval of 5 minutes, and the power output data is obtained from the micro-inverter EMA database.

The power data of the two PV panels is taking for a period of 10 days and the data is being analysed for the entire power output and time interval. In the following 3.4.2.2 below, the percentage difference between the experimental panel placed on the adjustable metal deck and the reference panel placed on the fixed metal deck is calculated (the air gap distance value is 12.5 cm).

$$\%_{\text{difference}} = \frac{P_{\text{Test}} - P_{\text{Ref}}}{P_{\text{Ref}}} \times 100\% \quad (3.4.2.2)$$

Where:

$\%_{\text{difference}}$ = Percentage difference between the power output of experimental PV panel and reference PV panel, %

P_{Test} = Power output of experimental PV panel, W

P_{Ref} = Power output of reference PV panel, W

By using the following equation 3.4.2.3 to convert power into energy, the power output of the PV panel can be further developed into electricity generation calibration.

$$E_{PV} = \frac{\sum P_{PV}}{1000 \times n} \times h \quad (3.4.2.3)$$

Where:

E_{PV} = Electricity generation of a PV throughout a day, kWh.

P_{PV} = Power output of the PV panel, W.

n = the number of data produced in the inverter.

h = hours, h

The difference in the percentage of electricity generation between two PV panels can be determined by adding the electricity generation of the reference PV panel and the experiment PV panels for 10 days following by using the equation in 3.4.2.4 below.

$$\%_{difference} = \frac{E_{Test} - E_{Ref}}{E_{Ref}} \times 100\% \quad (3.4.2.4)$$

Where:

$\%_{difference}$ = Percentage difference of electricity generation between the experimental PV panel and reference PV panel, %

E_{Test} = Electricity generated by experimental PV panel in a day, kWh

E_{Ref} = Electricity generated by reference PV panel in a day, kWh

The calibration result in Table 3.4.2.1 below show that the electricity generation of the experimental PV panel is about 3.67 % higher than electricity generation of the reference PV panel.

Table 3.4.2.1: Result of Electricity Generation Calibration at an air gap distance of 12.5 cm.

Air Gap =12.5 cm			
Date	E_{Ref} / kWh	E_{Exp} / kWh	% Difference / %
26/6/2020	0.8188	0.8439	3.0633
27/6/2020	0.7338	0.7574	3.2137
28/6/2020	0.8897	0.9195	3.3533
29/6/2020	0.6728	0.6934	3.0720
30/6/2020	0.8158	0.8449	3.5754
14/7/2020	0.9349	0.9695	3.6991
15/7/2020	0.8553	0.8891	3.9560
16/7/2020	0.7694	0.798	3.7149
17/7/2020	1.047	1.0918	4.2821
18/7/2020	0.8373	0.8747	4.4690
Total	8.3748	8.6822	3.67054

3.5 Experimental Measurement

After the PV panel and temperature sensors had been calibrated, the experimental is carried out by adjusting the metal deck to let the air gap distance between PV panel and the metal deck have an air gap distance increment ranging from 10.5 cm up to 20.5 cm. The PV module and ambient temperature can be obtained from the temperature data logger described in Section 3.1.2. Besides that, solar irradiance is obtained from the pyranometer at the weather station, and the power output obtained from the micro-inverter. The data were taken throughout 5 days with time from 9:30 a.m. and 5:30 p.m. with an air gap distance increment of 2 cm.

All data will be compiled and recorded in the example table in the Figure 3.5.1 below, with an interval of 5 minutes. The data is then further analysed in Section 3.6.

Date & Time	Solar Irradiance	Ambient Temperature	Reference Panel							Experiment Panel									
			Temperature				Power	Temperature				Power							
			LUC	RUC	LBC	RBC		Average	Average- AT	LUC	RUC		LBC	RBC	Average	Average- AT			

Figure 3.5.1: Table of measurement.

3.6 Experimental Analysis

After completing the measurement in Section 3.5, graphical analysis methods are performing by using various data variables in Section 3.5, as described in the next subsections below.

3.6.1 PV Average Temperature Analysis

To perform the average PV panel operating temperature analysis, the average operating temperature equation of each PV panel can be calculated in the equation 3.6.1.1 by using 4 DS18B20 temperature sensors in each panel.

$$T_{Avg} = \frac{T_{LUC} + T_{RUC} + T_{LBC} + T_{RBC}}{4} \quad (3.6.1.1)$$

Where:

T_{Avg} = Average operating temperature at for the each of PV panel, °C.

$T_{LUC}, T_{RUC}, T_{LBC}, T_{RBC}$ = Operating temperature recorded by each DS18B20 temperature sensor under each of PV panel, °C.

Then, use the following equations 3.6.1.2 and 3.6.1.3 to further average the average operating temperature of each of the reference PV panel and the experimental PV panel for one and five days.

$$T_{Avg,Day} = \frac{\sum T_{Avg}}{n} \quad (3.6.1.2)$$

Where:

$T_{Avg,Day}$ = Average operating temperature for the PV panel in a day, °C.

T_{Avg} = Average operating temperature at the PV panel, °C.

n = number of data produced through the day.

$$T_{Avg,Acc} = \frac{\sum T_{Avg,Day}}{n} \quad (3.6.1.3)$$

Where:

$T_{Avg,Acc}$ = Average operating temperature for the PV panel for 5 days, °C.

$T_{Avg,Day}$ = Average operating temperature for the PV panel in a day, °C.

n = number of days.

The final relative difference in the averaging operating temperature of the PV panels between experiment PV panel and reference PV panel and can be calculated in the following equation 3.6.1.4.

$$\Delta T_{Avg,Acc} = T_{Avg,Acc,Exp} - T_{Avg,Acc,Ref} \quad (3.6.1.4)$$

Where:

$\Delta T_{Avg,Acc}$ = Relative Difference between operating temperature for the experiment and reference PV panel for 5 days, °C.

$T_{Avg,Acc,Exp}$ = Average operating temperature at experimental PV panel for 5 days, °C.

$T_{Avg,Acc,Ref}$ = Average operating temperature at reference PV panel for 5 days, °C.

Then, the final relative difference in the average operating temperature between experiment PV panel and reference PV panels is plotted against the air gap distance and the effects of air gap distance to the average operating temperature of the PV panels.

3.6.2 PV Electricity Generation Analysis

In order to calculate the power output on the experimental PV panel based on the reference PV panel and experimental PV panel operating temperature, the equation in 2.1.3 is modified to the following equation 3.6.2.1 to determine the calculated power output.

$$P_{Cal} = P_{Ref}(1 + \gamma(T_{Ref} - T_{Exp})) \quad (3.6.2.1)$$

Where:

P_{Cal} = Calculated Power output based on temperature coefficient, W

P_{Ref} = Power output based on microinverter at the reference panel, W

γ = Temperature coefficient of Power, %/°C, which is -0.4112 %/°C shown in Section 3.2.1

T_{Ref} = Average operating temperature the reference PV panel, °C.

T_{Exp} = Average operating temperature for the experimental PV panel, °C.

In order to analyse the calculated output of PV electricity generation in the experimental PV panel, it is necessary to apply an equation for calculating a day's electricity generation based on calculated power output based on the equation 3.6.2.1 in 3.4.2.3. Next, use the equation 3.6.2.2 to calculate the cumulative calculated electricity generation of the experiment PV panel and the reference PV panel for over 5 days.

$$E_{Total} = \sum E_{day} \quad (3.6.2.2)$$

Where:

E_{Total} = Total Electricity generation in 5 days on the PV panel, kWh

E_{Days} = Electricity generated by the PV panel in a day, kWh

In addition, using the equation 3.4.2.4, the percentage difference of calculated electricity generation over five days between experiment PV panel and the reference PV panel is calculated. Next, use the equations 3.4.2.3, 3.4.2.4

and 3.6.2.2 to calculate the percentage difference of measured electricity generation between experiment PV panel and the reference panel for over 5 days.

Last but not least, by plotting two graphs, which are the graph of calculated or measured percentage difference of electricity generation between experiment PV panel and the reference PV panel versus air gap distance and distance to determine the effects of air gap to the electricity generation of the PV panel.

3.6.3 Ross Coefficient Analysis

The original Ross model for determine the operating temperature of a PV panel by using the ambient temperature and solar irradiance one the PV panel is in example equation 2.1.4. The equation stated before has been modified to equation 3.6.3.1 to plot the relationship between the temperature difference between operating temperature of the experimental PV panel or reference PV panel and ambient temperature versus the solar irradiance. By using the graph stated above, the Ross coefficient value can be determined based on equation 3.6.3.1.

$$\Delta T_{PV} = kG_M \quad (3.6.3.1)$$

Where:

ΔT_{PV} = Difference between PV Module temperature and Ambient Temperature, °C

k = Ross coefficient that determine the slope between the temperature and irradiance level, °C m²/W (Ross, 1976)

G_M = Irradiance on PV module, W/ m²

The Ross coefficient value of each air gap distance can be plotted with the air gap distance between the PV panel and the metal deck to determine the influence of air gap to the Ross coefficient value of the PV panel.

3.6.4 Cost Analysis

To determine whether the optimization of the air gap distance in the BAPV system is economically possible, cost-effective analysis methods will be used throughout the study to evaluate.

First, the cost of installing aluminium hooks to increase the air gap distance in BAPV systems is known and listed. Next, assume the number and electricity generation capacity of the BAPV system. From the earlier hypothetical statement, the number of hooks require for a BAPV system can be calculated in the following equation 3.6.4.1.

$$n_{hook} = \frac{P_{BAPV}}{P_{panel}} \quad (3.6.4.1)$$

Where:

n_{hook} = Number of hooks required for whole BAPV System.

P_{BAPV} = Electricity generation capacity for a BAPV system, kW

P_{panel} = Electricity generation capacity for a single PV Panel, W

The increment cost of the number piece of hook compared to the standard installation of 12.5 cm air gap distance from the cost of installing aluminium hooks to increase the air gap distance in BAPV systems is calculated in the following equation 3.6.4.2.

$$RM_{invest} = n_{hook} \times RM_{hook} \quad (3.6.4.2)$$

Where:

RM_{invest} = Total price increment on a BAPV System, RM

n_{hook} = Number of hooks required for whole BAPV System.

RM_{hook} = Price increment per hook based on reference PV panel (12.5 cm), RM

Besides that, the cost-effective analysis also assumes the initial performance ratio of the PV panels is usually 0.8. With ventilation by increasing the air gap distance between PV panels and metal deck, the percentage increment of electricity generation can be seen based on the electricity generation analysis. The improved performance ratio based on electricity generation analysis is then calculated in equation 3.6.4.3.

$$PR_{air\ gap} = PR_{initial} + \frac{\%difference}{100} \quad (3.6.4.3)$$

Where:

$PR_{air\ gap}$ = Performance Ratio for a single PV Panel with improved performance by using extra air gap distance.

$PR_{initial}$ = Performance Ratio for a single PV Panel with commercial air gap distance (12.5 cm), which is 0.8

$\%difference$ = Percentage difference of electricity generation between the experimental PV panel and reference PV panel, %

Taking a site in Malaysia with moderate solar irradiation, the annual peak sun hours (PSH) is 1700 hours, with that, an extra electricity can be produced in a year due to cooling effects can be calculated in equation 3.6.4.4 below:

$$E_{Year} = PSH \times P_{BAPV} \times (PR_{air\ gap} - PR_{initial}) \quad (3.6.4.4)$$

Where:

E_{Year} = Extra electricity generation in a year due to cooling effects, kWh

PSH = Peak Sun Hour, hour, which is assumed as 1700 hours

P_{BAPV} = Electricity generation capacity for a BAPV system, kW

$PR_{air\ gap}$ = Performance Ratio for a single PV Panel with improved performance by using extra air gap distance.

$PR_{initial}$ = Performance Ratio for a single PV Panel with commercial air gap distance (12.5 cm), which is 0.8

Most of the Projects granted with incentives or electricity sold under the Power Purchasing Agreement (PPA) last of 21 years, an average degradation rate of solar panel is 0.55 % per year, The degradation rate will bring a compound factor of 0.925 of the first electricity generation. Therefore, the total extra electricity generation by increment of air gap distance in 21 years are using the equation 3.6.4.5 below:

$$E_{total} = 21 \text{ years} \times DF \times E_{Year} \quad (3.6.4.5)$$

Where:

E_{total} = Total extra electricity generation in 21 years, kWh

DF = Compound degradation factor in 21 years, which is 0.925

E_{Year} = Extra electricity generation in a year due to cooling effects, kWh

The NEM policies states that highest electricity tariff for domestic consumers is 0.546 /kWh (Tenaga Nasional Berhad, 2020). Hence, the total extra money earn in 21 years can be calculated by multiplying by total extra electricity generation in 21 years with tariff gain per kilowatt hour by using the equation 3.6.4.6.

$$RM_{gained} = E_{total} \times Tariff \quad (3.6.4.6)$$

Where:

RM_{gained} = Total extra money earned in 21 years, RM

E_{total} = Total extra electricity generation in 21 years, kWh

$Tariff$ = Tariff gained per kilowatt hour, which is RM 0.546/ kWh. (Tenaga Nasional Berhad, 2020)

The total extra money gained of each increment of air gap distance can be plotted with the air gap distance between the PV panel and the metal deck to determine the impact of air gap distance on total extra money gained on the PV panel.

3.7 Experimental Planning

Before continuing with the experimental program, make a Gantt chart to ease planning and scheduling. Besides that, the Gantt chart also required to keep track of the experiment so that it would not miss any critical task. Table 3.7.1 shows the Gantt chart for Part 1 of the project.

According to the first half of project progress in the following Table 3.7.1, several articles have been studied, and the overview of process method

had been completed. After inspecting and measuring the mechanical roof deck and, it was concluded that the project will use mechanical structure described in Section 3.1.1. In addition, the components used in this research have been found and noted also bought in the Section 3.2. Moreover, the hardware construction and software programming of Raspberry PI temperature data logger is done as described in Section 3.1.2.

Table 3.7.1: Gantt chart of the first half of the project.

No.	Project Activities	W1	W2	W3	W4	W5	W6	W7	W8	W9	W10	W11	W12	W13	W14
M1	Article Research														
M2	Research Proposal														
M3	Mechanical Structure Measurement														
M4	Component Determination and Buy Components														
M5	Raspberry Pi Data Logger Circuits Building														

Table 3.7.2 shows the Gantt chart for Part 2 of the project. In the second part of project, the temperature sensors and PV panels have been calibrated by the steps in Sections 3.4.1 and 3.4.2. Necessary data collection such as collect solar irradiance from weather station, ambient and PV panels operating temperature from Raspberry PI data logger and power output of the PV panels is getting from micro-inverter EMA web server is done as in Section 3.5. Finally, as described in Section 3.6, perform data analysis such as average temperature analysis, electricity generation analysis and Ross coefficient value analysis.

Table 3.7.2: Gantt chart of the second half of the project.

No.	Project Activities	W1	W2	W3	W4	W5	W6	W7	W8	W9	W10	W11	W12	W13
M1	Temperature Sensor Calibration	█	█											
M2	Installation of PV System onto Metal Deck	█	█											
M3	PV Panel Calibration	█	█	█										
M4	Air Gap Determination and Adjustment	█	█	█	█	█	█	█	█					
M5	Cell and Ambient Temperature Collection	█	█	█	█	█	█	█	█	█				
M6	PV Panel Output Power Collection	█	█	█	█	█	█	█	█	█	█			
M7	Solar Irradiance Collection	█	█	█	█	█	█	█	█	█	█	█		
M8	Average Temperature Analysis			█	█	█	█	█	█					
M9	Electricity Generation Analysis			█	█	█	█	█	█					
M10	Ross Coefficient Analysis			█	█	█	█	█	█					

3.8 Summary

In a nutshell, metal deck mechanical structure with adjustable height is re-measured to hold the metal deck roof and PV panels are placed side-by-side and connecting to the same microinverter; one with adjustable air gap distance, another one with a fixed air gap distance of 12.5 cm (commercial air gap distance). The Raspberry Pi data logger is designed to record data on the ambient temperature and the operating temperatures of PV panels. Before starting to collect data, temperature sensors and PV panels must be calibrated. After collecting the data from various sources, then data must be analysed.

CHAPTER 4

RESULTS AND DISCUSSION

4.1 Introduction

As mention in the earlier chapter, according to the methods of data collection and data analysis, a large amount of useful data has been recorded when conducting research experiments. The collected data will be displayed in graphs and tables for further analysis.

The original data was collected from three source. Solar irradiance data are collected from the weather station at UTAR, Power data are collected from micro-inverter EMA web server and last but not least, ambient temperature and solar PV operating temperature data are collected from Raspberry Pi Data Logger. All data is collected on the roof of UTAR KB block. During the analysis as in Section 3.6, the results is explained in the figures and tables in the following sections.

4.2 Average Temperature Analysis

According to the output power of the micro-inverter, the average operating temperature of two PV panels is obtained and analysed at intervals of 5 minutes within 5 days. The results are analysed as following Section 3.6.1. All the results are listed in Appendix B. The following Table 4.2.1 lists the relative result of average operating temperature in the experiment PV panel relatively to the reference PV panel and the experimental air gap distance.

Table 4.2.1: Table of experimental air gap and operating temperature in the experiment PV panel relatively to reference PV panel, $\Delta T_{Avg,Acc}$

Experimental Air gap, d_f /cm	$\Delta T_{Avg,Acc}$ / °C.
10.5	1.0816
12.5	1.0007
14.5	0.0954
16.5	-0.2096
18.5	-0.4889

20.5	-0.5177
------	---------

Based on Table 4.2.1, the relationship between the average operating temperature in the experiment PV panel relatively to the reference PV panel versus experimental air gap distance is drawn in Figure 4.2.1 below.

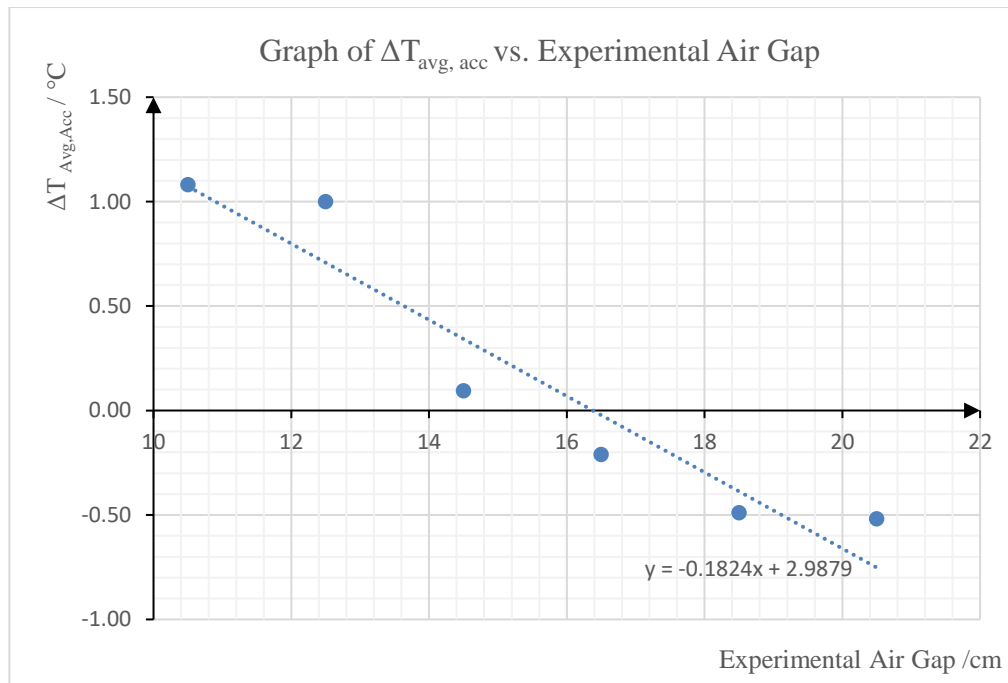


Figure 4.2.1: Graph of average operating temperature in the experiment PV panel relatively to the reference PV panel versus experimental air gap.

From the Figure 4.2.1 above, it is important not to overlook that during 12.5 cm air gap when the experimental air gap is same with the reference air gap, there is an error of a positive of 1 °C at the average operating temperature in the experiment PV panel relatively with the reference PV panel. This result differs from the assumption that when the air gap between the PV panel and the metal deck is the same, the temperature in the experimental panel relative with the reference panel should be 0 °C.

Therefore, in order to eliminate the above error, the offset method is used to make the temperature in the experimental PV panel relative with reference PV panel for 5 days under the 12.5 cm experimental air gap is equal to zero. To implement this method, the following equation 4.2.1 is used for shifting purpose.

$$\Delta T_{shifted,Avg,Acc} = \Delta T_{Avg,Acc} - \Delta T_{err} \quad (4.2.1)$$

$\Delta T_{shifted,Avg,Acc}$ = Shifted operating temperature relative difference between experimental PV panel and reference PV panel for 5 days, °C.

$\Delta T_{Avg,Acc}$ = Operating temperature relative difference between for the experimental PV panel and reference PV panel for 5 days, °C.

ΔT_{err} = Error occurred in 12.5 cm air gap at Table 4.2.1, which is 1.0007 °C.

Table 4.2.2 shows the data results of the shifted operating temperature in the experiment PV panel relative to the reference PV panel based on Table 4.2.1. Correspondingly, the graph of the shifted operating temperature difference in the experiment PV panel relatively to the reference PV panel versus experimental air gap based on Table 4.2.2 is plotting in Figure 4.2.2.

Table 4.2.2: Table of the experimental air gap and shifted operating temperature in the experimental PV panel relative to reference PV panel.

Experimental Air gap, d_f /cm	$\Delta T_{shifted,Avg,Acc}$ / °C.
10.5	0.0809
12.5	0
14.5	-0.9053
16.5	-1.2103
18.5	-1.4896
20.5	-1.5184

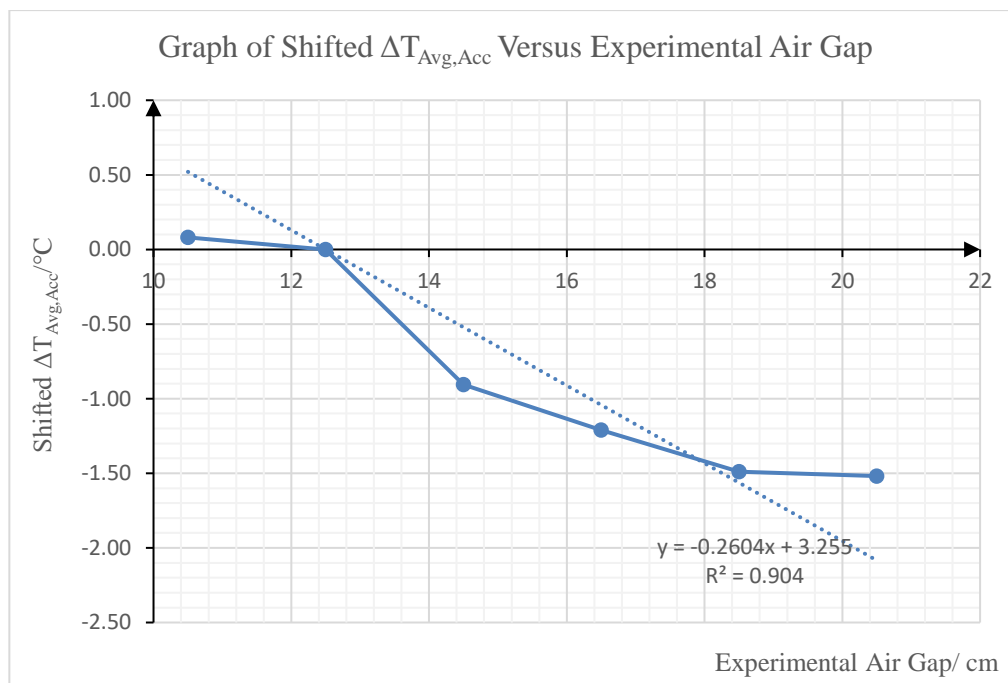


Figure 4.2.2: Graph of shifted average operating temperature in the experiment PV panel relatively to the reference PV panel versus experimental air gap.

As can be seen from the Figure 4.2.2, The average operating temperature of PV module becomes increasing lower relatively to that of reference panel when the air gap distance increases from 12.5 cm towards 20.5 cm. Contrary, it becomes higher when air gap distance reduces from 12.5 cm to 10.5 cm. When air gap distance reduces from 12.5 cm to 10.5 cm, the average operating temperature compared to the reference panel increase to 0.08 $^{\circ}C$. Contrary, when air gap distance increase from 12.5 cm to 20.5 cm, the average operating temperature compared to the reference panel decrease to 1.5 $^{\circ}C$.

In addition, based on the linear regression equation in Figure 4.2.2, the operating temperature in experiment PV panel relatively to the reference PV panel is lower by about 0.26 $^{\circ}C$ every 1 cm air gap increase and vice versa. This fact proves that a larger air gap between the metal deck and PV panel provides better ventilation to the PV panel as it lets the operating temperature on the PV panel decrease.

4.3 Electricity Generation Analysis

According to the output power of the micro-inverter, the calculated output of PV electricity generation in the experimental PV is completed according to

equations 3.6.2.1 and 3.6.2.2 within 5 days. Table 4.3.2 shows the result of electricity generation calculated based on output power of reference PV panel in Appendix C and Table 3.4.2.1.

Table 4.3.1: Table of the experimental air gap, electricity generation by reference PV panel and calculated experiment PV panel also electricity generation calculated percentage difference between experimental PV panel and reference PV Panel, $\%E_{Theo}$.

Experimental Air Gap, d_f / cm	E_{Ref} / kWh	E_{Cal} / kWh	$\%E_{Cal}$
10.5	3.606	3.5858	-0.5602
12.5	8.3748	8.3327	-0.5027
14.5	4.2968	4.2951	-0.0396
16.5	3.9445	3.9484	0.0989
18.5	4.9417	4.953	0.2287
20.5	5.1836	5.1957	0.2334

Similarly, Table 4.3.2 shows the result of measured electricity generation calculated based on output power of reference and experimental PV panel in Appendix C and Table 3.4.2.1.

Table 4.3.2: Table of the experimental air gap, electricity generation by reference PV panel and measured experiment PV panel also electricity generation percentage difference between actual experimental PV panel and reference PV Panel, $\%E_{Theo}$.

Experimental Air Gap, d_f / cm	E_{Ref} / kWh	$E_{Exp,Theo}$ / kWh	$\%E_{Theo}$
10.5	3.606	3.7318	3.4886
12.5	8.3748	8.6822	3.6705
14.5	4.2968	4.5006	4.7431
16.5	3.9445	4.1087	4.1628
18.5	4.9417	5.1729	4.6786
20.5	5.1836	5.4414	4.9734

From the above Tables 4.2.1 and 4.2.2, it can be inferred that when the experimental air gap increases, the 5-day electricity generation percentage difference between the calculated or measured experimental PV panel and the reference PV panel will increase. However, it is important not to overlook that during 12.5cm air gap when the experimental air gap is same with the reference air gap, there about -0.5 % difference error between the calculated experimental PV panel electricity generation output and reference PV panel electricity generation output. In addition, the error of percentage difference between the measured experimental PV panel and the reference PV panel electricity generation is 3.67%. These results differ from the assumption that when the air gap between the PV panel and the metal deck is the same, the electricity generation percentage difference should be zero.

Therefore, in order to eliminate the above error, the offset method is used to make the 5-day electricity generation percentage difference between the calculated or measured experimental PV panel and the reference PV panel under the 12.5 cm experimental air gap is equal to zero. To implement this method, the following equation 4.3.1 is used for offset purpose.

$$\%E_{Act} = \%E_{Rec} - \%E_{err} \quad (4.3.1)$$

Where:

$\%E_{Act}$ = Actual electricity generation percentage difference, %

$\%E_{Rec}$ = Recorded electricity generation percentage difference, %

$\%E_{err}$ = Electricity output percentage error from the reference air gap, which is -0.5027 % in Table 4.3.1 and 3.6705 % in Table 4.3.2/ %

Table 4.3.3 shows the data results of the shifted electricity percentage generation difference between calculated or measured experiment PV panel and reference PV panel based on Tables 4.4.1 and 4.4.2. Correspondingly, the relationship between the shifted electricity percentage generation difference between calculated or measured experiment PV panel and reference PV panel based on Table 4.3.3 and experimental air gap is shown Figure 4.3.1.

Table 4.3.3: Table of the experimental air gap and shifted electricity generation percentage increment between calculated or measured experimental PV panel and reference PV Panel, $\%E_{Theo,inc}$.

Experimental Air gap, d_f /cm	$\%E_{Cal}$ /%	$\%E_{Act}$ / %
10.5	-0.0575	-0.1819
12.5	0	0
14.5	0.4631	1.0725
16.5	0.6016	0.4922
18.5	0.7314	1.0080
20.5	0.7361	1.3028

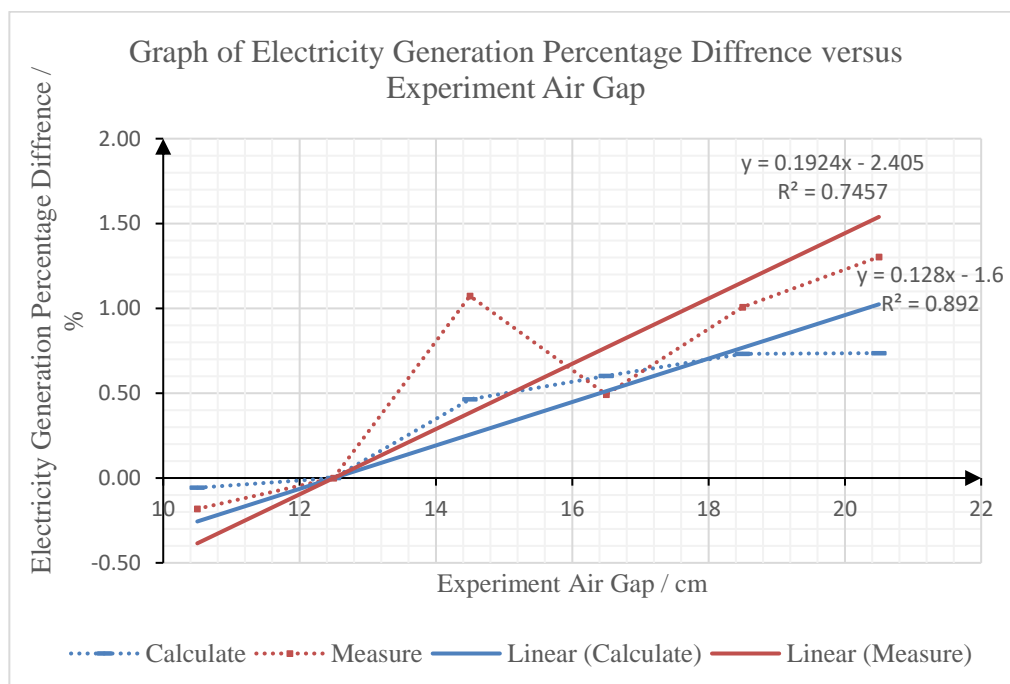


Figure 4.3.1: Graph of Electricity Generation Percentage Difference Versus Experimental Air Gap.

By looking at Figure 4.3.1, it can be deduced that there is an increasing graphical trend in the electrical generation percentage difference for both calculated and measured. As in the Figure 4.3.1 above, the experiment air gap is equal 20.5 cm, the calculated electricity generation percentage difference is increase to 0.74 %, while the measured electricity generation percentage has increase to 1.3 %. It can be concluded that the measured electricity generation

percentage difference is higher than the calculated electricity generation percentage.

Besides that, there is a difference in the slope in the linear regression equation in the calculated electricity generation percentage difference and measured electricity generation percentage difference. It shows that an increment of 1 cm air gap will have a 0.12 % increment in the calculated electricity generation percentage difference, but it will have a increment of 0.19 % in the measured electricity generation percentage.

In addition, the measured electricity generation in air gap 14.5 cm increase to 1.07 %, which is consider an inaccuracy on measured electricity generation graph.

4.4 Ross Coefficient Analysis

Figure 4.4.1 shows an example of the relationship between of the difference between operating temperature of PV panels and ambient temperature versus the solar irradiance when the air gap distance of the reference PV panel and the experimental PV panel is the same, which is 12 cm.

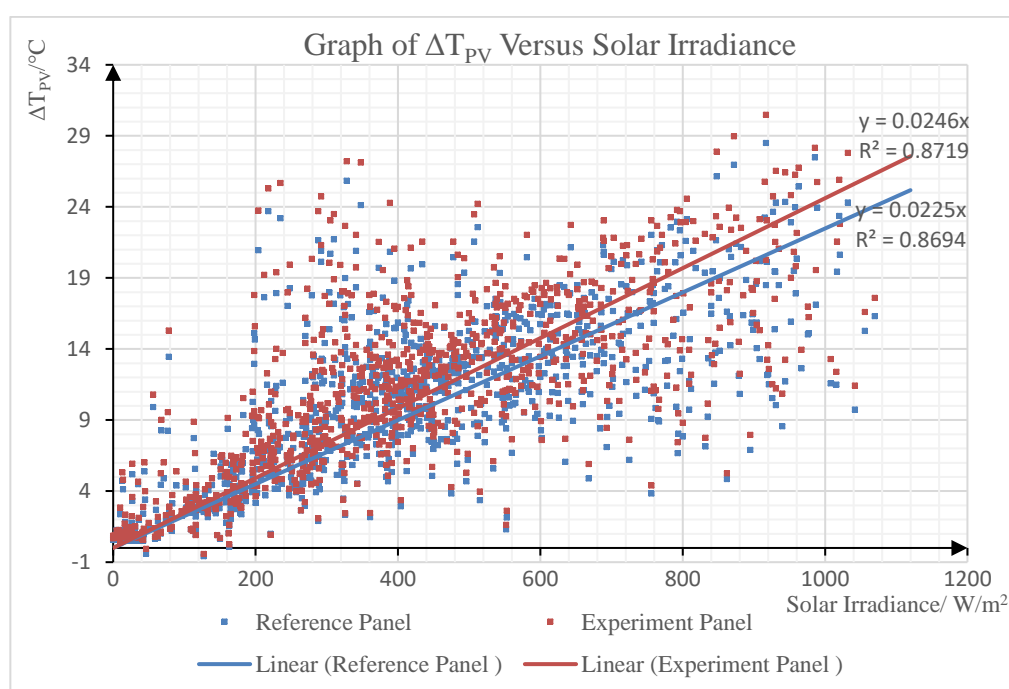


Figure 4.4.1: Graph of ΔT_{PV} versus Solar Irradiance for Reference air gap = 12.5 cm and Experimental Air Gap = 12.5 cm.

It can be inferred from the Figure 4.4.1 that when the solar irradiance increase, the temperature difference between both PV panels and the ambient temperature is increase. Besides that, based on the linear regression equation in Figure 4.4.1, That when two air gaps are the same during calibration process, the Ross coefficient values (which is the linear regression slope values) in the reference PV panel and experimental PV panel is different. This is different from the assumption that when the air gap between the PV panel and metal deck for both PV panel, the values of the Ross coefficient is the same. This is because, as described in Section 4.2, there is a difference in operating temperature between the experimental PV panel and reference PV panel.

Next, Appendix D shows five similar graphs of the relationship between of the difference between operating temperature of PV panels and ambient temperature versus the solar irradiance in each air gap. According to the results in Figure 4.4.1 and Appendix D, the Ross coefficient values in the reference PV panel and the experimental PV panel can be summarised in the following Table 4.4.1.

Table 4.4.1: Table of experimental air gap, reference PV panel Ross coefficient value, k_{ref} and experimental PV panel Ross coefficient value, k_{Exp} .

Experimental Air gap, d_f /cm	k_{ref} , °C m ² /W	k_{Exp} , °C m ² /W
10.5	0.0232	0.0259
12.5	0.0225	0.0246
14.5	0.0243	0.0245
16.5	0.0222	0.0217
18.5	0.0209	0.0201
20.5	0.0203	0.0195

Therefore, in order to eliminate the error occurs in the Ross coefficient value to meet the assumption based on the explanation in Figure 4.4.1, the Ross coefficient value difference between the experimental PV panel and reference PV panel is calculated based on the result in Table 4.4.1 and the following equation 4.4.1:

$$\Delta k = k_{exp} - k_{ref} \quad (4.4.1)$$

Where:

Δk = Ross coefficient difference between experimental PV panel and reference PV panel, °C m²/W

k_{exp} = Ross coefficient values in the experimental PV panel based on Table 4.4.1, °C m²/W.

k_{ref} = Ross coefficient values in the reference PV panel based on Table 4.4.1, °C m²/W.

Next, offset method is used to letting the Ross coefficient difference between experimental PV panel and reference PV panel when the 12.5 cm air gap is equal to 0 as shown in following equation 4.4.2. In addition, equation 4.4.3 is used to calculate the final Ross coefficient value in the experiment PV panel.

$$\Delta k_{shift} = \Delta k - \Delta k_{12.5cm} \quad (4.4.2)$$

Where:

Δk_{shift} = Shifted Ross coefficient difference between experimental PV panel and reference PV panel, °C m²/W

Δk = Ross coefficient difference between experimental PV panel and reference PV pane, °C m²/W.

$\Delta k_{12.5cm}$ = Ross coefficient difference between experimental PV panel and reference PV panel at 12.5cm

$$k_f = k_{exp} + \Delta k_{shift} \quad (4.4.3)$$

Where:

k_f = Final Ross coefficient value on experimental PV panel, °C m²/W.

k_{exp} = Ross coefficient values in the experimental PV panel based on Table 4.4.1, °C m²/W.

Δk_{shift} = Shifted Ross coefficient difference between experimental PV panel and reference PV panel, $^{\circ}\text{C m}^2/\text{W}$

Table 4.4.2 shows the result of three calculations based on the equations in 4.4.1, 4.4.2 and 4.4.3. The graph of the final Ross coefficient value is plotted together with the experimental air gap in Figure 4.4.2.

Table 4.4.2: Table of the experimental air gap, Ross coefficient difference between experimental PV panel and reference PV panel, Δk , shifted Ross coefficient difference between experimental PV panel and reference PV panel, Δk_{shift} and final Ross coefficient value on experimental PV panel, k_f

Experimental Air gap, d_f/cm	Δk , $^{\circ}\text{C m}^2/\text{W}$	Δk_{shift} , $^{\circ}\text{C m}^2/\text{W}$	k_f , $^{\circ}\text{C m}^2/\text{W}$
10.5	0.0027	0.0006	0.0265
12.5	0.0021	0	0.0246
14.5	0.0002	-0.0019	0.0226
16.5	-0.0005	-0.0026	0.0191
18.5	-0.0008	-0.0029	0.0172
20.5	-0.0008	-0.0029	0.0166

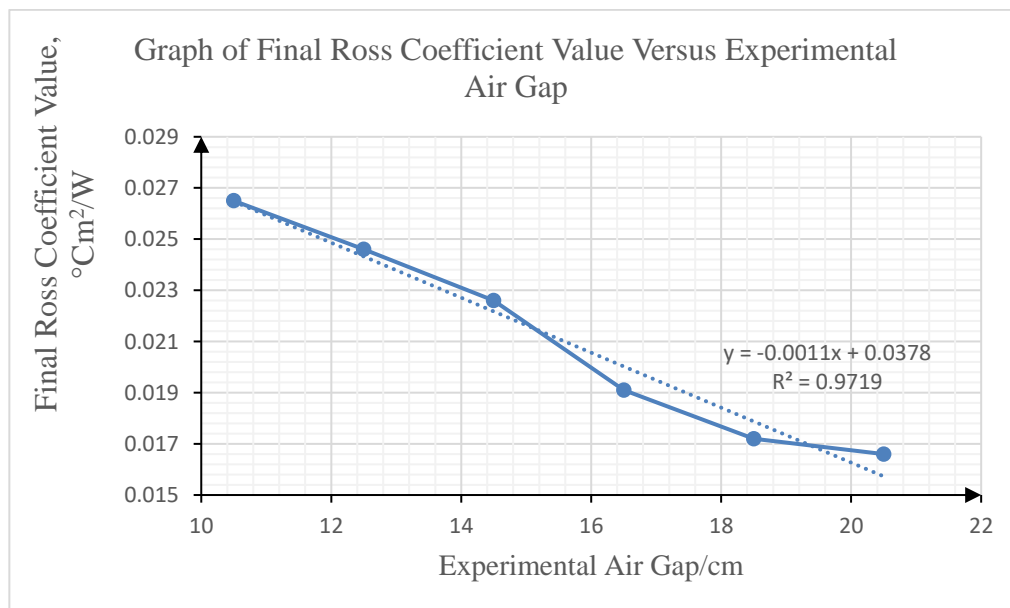


Figure 4.4.2: Graph of Final Ross Coefficient Values versus experimental air gap.

The result shows that when the experimental air gap increases, the Ross coefficient decreased. The results also show that when air gap distance increase from 12.5 cm to 20.5 cm, the shifted Ross coefficient value is decrease from 0.0246 °C m²/W to 0.0166 °C m²/W. In addition, based on Figure 4.4.1 that through linear regression equation, when the air gap increases by 1 cm, the value of Ross coefficient decreases by 0.0011 °C m²/W. This further proves that a large air gap between the metal deck and PV panel provides better ventilation to the PV panel as it lets the operating temperature on the PV panel decrease. The heat produced by the PV during high solar irradiance can ventilate more easily with large air gap distance.

4.5 Cost Analysis

Based on the cost analysis method in the Section 3.6.4, the actual cost of aluminium hook is listed out in the Table 4.5.1 below.

Table 4.5.1: Material Cost for aluminium hook and price increment per aluminium hook based on reference air gap.

Experimental Air gap / cm	Price for one Hook / RM	Average hook use for one PV Panel	Price for hook in one PV panel / RM	Price increment per hook Based on Reference / RM
12.5	5.39	1.867	10.06	0
14.5	5.97		11.15	1.09
16.5	6.55		12.22	2.16
18.5	6.94		12.95	2.89
20.5	7.32		13.66	3.6

Suppose a 90-kW system has 300 of 300 W panels. Therefore, according to equation 3.6.4.1, 300 hooks are required. By using equation 3.6.4.2, based on hook price increment of in each air gap increment in Table 4.5.1 ,and comparing with a standard installation of 12.5 cm air gap, the extra cost of 300 hooks is shown in Table 4.5.2. Next, the relationship between the experimental air gap and the extra cost on a 90-kW BAPV system is plotted in Figure 4.3.1.

Table 4.5.2: Table of experiment air gap and Total price Investment on a 90 kW BAPV System.

Experimental Air gap / cm	Extra Cost on a 90 kW BAPV System / RM
12.5	0
14.5	325.80
16.5	648
18.5	866.29
20.5	1080

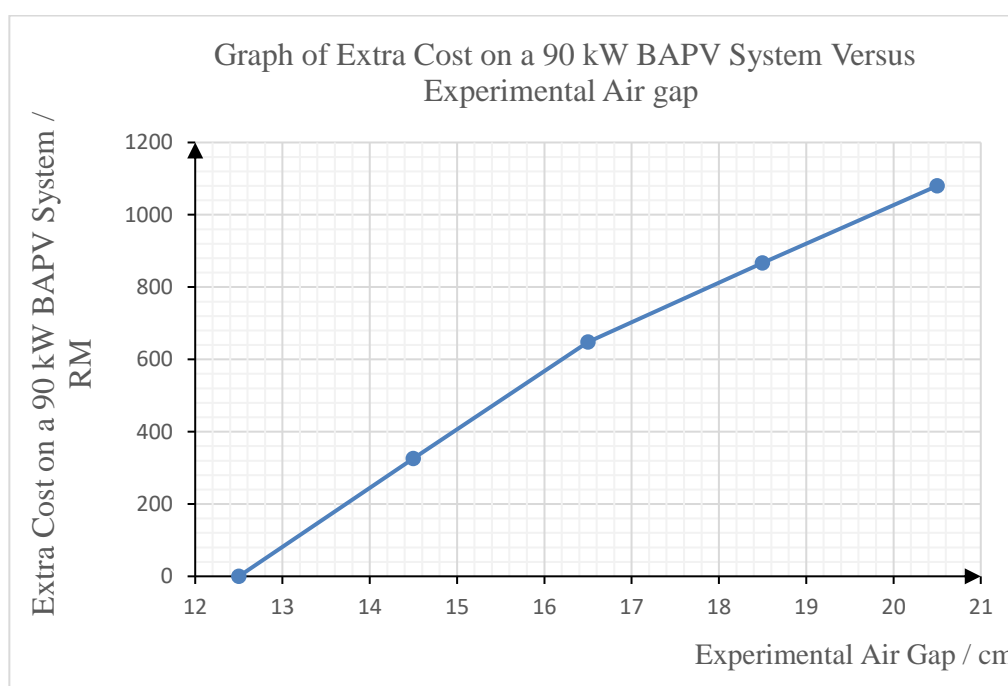


Figure 4.5.1: Graph of Extra Cost on a 90 kW BAPV system versus Experimental air gap.

The result shows that when the experimental air gap increases, the extra cost on a 90-kW BAPV system is increase. This is because the metal used for having more air gap in the BAPV system is increase. Next, based on the equations 3.6.4.3 and 3.6.4.4, also the actual electricity percentage difference between experiment PV panel and reference PV panel in Table 4.3.3, calculate the additional electricity that can be generated in a year with the improvement performance ratio. The results are shown in Table 4.5.3.

Table 4.5.3: Table of experiment air gap, improved performance Ratio for a PV system, and extra electricity generation in a year.

Experimental Air gap / cm	Improved Performance Ratio for a PV system	Extra electricity generation in a year /kWh
12.5	0.8000	0
14.5	0.8107	1640.93
16.5	0.8049	753.07
18.5	0.8101	1542.24
20.5	0.8130	1993.28

Next, based on the equation 3.6.4.5, the total additional electricity generation in 21 years is calculated by using the additional electricity generation in a year in Table 4.5.3 above. The additional electricity income in 21 years is also calculated based on the equation 3.6.4.6. The results are shown in Table 4.5.4. Correspondingly, Figures 4.5.2 plots the relationship between the additional electricity income in 21 years and the experimental air gap.

Table 4.5.4: Table of experiment air gap, extra electricity generation in 21 years, and extra electricity income in 21 years.

Experimental Air gap / cm	Extra electricity generation in 21 years/ kWh	Extra electricity income in 21 years/ RM
12.5	0	0.00
14.5	31874.97	17403.73
16.5	14628.31	7987.06
18.5	29958.01	16357.07
20.5	38719.54	21140.87

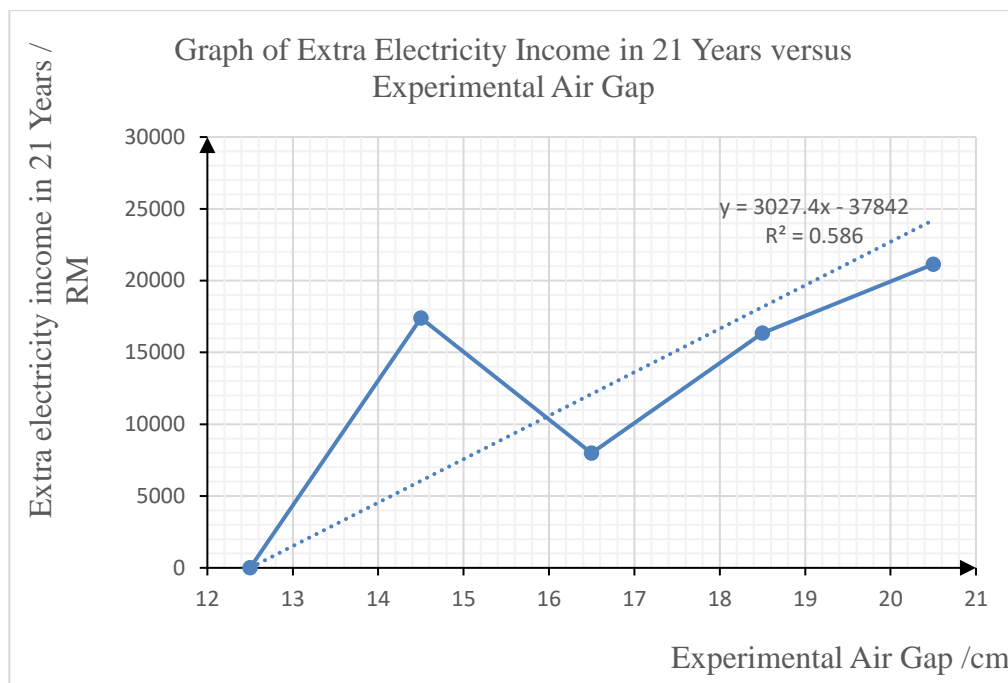


Figure 4.5.2: Graph of extra Electricity Income in 21 years versus Experimental Air gap.

The result in Figure 4.5.2 shows that when the experimental air gap increases, the additional electricity revenue in 21 years will generally increase. However, it is shown that the 14.5 cm air gap, the extra electricity income in 21 years has some inaccuracy. This is due to the inaccuracy during electricity generation analysis described in Section 4.3.1.

Based on the Figures 4.5.1 and 4.5.2 above, It can be concluded that an extra investment on RM 1080 for increasing the air gap from standard installation of the 12.5 cm to air gap of 20.5 cm can bring an extra revenue of RM 21140.87 for a 90 kW PV system in 21 years. In addition, based on Figure 4.5.2, through linear regression equation, when the air gap increases by 1 cm, an additional income of RM 3027.40 can be obtained for a 90 kW PV system in 21 years.

4.6 Summary

In short, PV panels operate a lower temperature with a larger air gap distance, because heat release into the surrounding environment at a faster rate. It not only reduces the operating temperature difference between experimental PV panel and reference PV panel, but also reduces Ross coefficient values of the

experimental PV panel. Besides, the electricity generation by PV panel increases either calculated or measured with the increase of the air gap. In addition, if the electricity is sold to utility companies based on tariff rate, the increased electricity generation will provide more revenue.

CHAPTER 5

CONCLUSIONS AND RECOMMENDATIONS

5.1 Conclusions

Through this project, a Raspberry Pi temperature sensor data logger had been built, and the operating temperature of the PV panel and ambient temperature were measured at different air gap distance by using the Raspberry Pi Data logger circuit. The relation between the operating temperature, electricity generation and Ross coefficient value with different air gap distance have been analysed and modelled.

The average operating temperature of PV module becomes increasing lower relatively to that of reference panel when the air gap distance increases from 12.5 cm towards 20.5 cm. Contrary, it becomes higher when air gap distance reduces from 12.5 cm to 10.5 cm. When the air gap distance reduces from 12.5 cm to 10.5 cm, the average operating temperature of PV module compared to the reference panel increase to 0.08 °C. Contrary, when air gap distance increase from 12.5 cm to 20.5 cm, the average operating temperature of PV module compared to the reference panel decrease to 1.5 °C.

Besides, as the air gap increases, the difference in the percentage of total electricity generation output between the reference PV panel and experimental PV panel within 5 days has an increasing pattern. The total electricity generation percentage difference between the reference PV panel and the experimental PV panel in 5 days increased from -0.2 % when the air gap is 10.5 cm to 1.3 % when the air gap is 20.5 cm.

On the other hand, when the air gap increases, the Ross coefficient value for the experimental PV panel decreases. The value of the Ross coefficient value is reduced form 0.0265 °C m²/W with an air gap of 10.5 cm to 0.0166 °C m²/W with an air gap of 20.5cm.

In addition, a cost analysis was performed to calculate the extra income can be obtained from electricity selling and the additional cost of the mechanical air gaps from the increment of air gap distance. It shows that for air gap distance of 20.5 cm, a PV system of 90 kW can gain extra energy profit of RM 21140.87

through 21 years of project lifetime under Net Energy Metering (NEM) scheme available in Malaysia.

These findings provide the important insights that natural ventilation plays a huge role in dissipating the heat from PV panels, which will reduce temperature efficiency loss of PV panels. Therefore, as the air gap increases, the electricity generation output performance of the PV panel is better also will generate more income if these extra electricity generation is selling to electricity utilities company such as Tenaga Nasional Berhad (TNB). In the nutshell, all project objectives had been achieved.

5.2 Recommendations for future work

To remotely check and obtain temperature data, it is recommended to add the existing Raspberry Pi temperature data logger circuit with NodeMCU ESP 8233 microcontroller as a server function. This is because there is a limitation with Raspberry Pi alone as it needs a Wi-Fi connection for constantly uploading data to website server and the location of the data taken is remote as it does not have any Wi-Fi connection.

In order to improve the accuracy of the collected result, it is recommend to conduct experiments on more PV panels; one as reference PV panel with a reference air gap distance, and others as experiment PV panels with a different air gap distance. This is because data can be collected at same time, and long-term electricity generation and operating temperature analysis for PV panels can be performed under different air gaps.

Besides that, solar irradiance sensor is recommended to place beside the PV panel to record the solar irradiance data to increase the accuracy as it placed at close vicinity with the panel comparing to the weather station which is 7 meters away.

Last but not least, wind load analysis on the PV mechanical structure is an interesting area for further research. This is because as higher the air gap distance between the PV panel and metal deck structure, the wind may blow away the structure supports the PV panel then creating a safety issue to the consumer after installing the BAPV system on the rooftop.

REFERENCES

- Amelia, A.R., Irwan, Y.M., Leow, W.Z., Irwanto, M., Safwati, I. and Zhafarina, M., 2016. Investigation of the effect temperature on photovoltaic (PV) panel output performance. *International Journal on Advanced Science, Engineering and Information Technology*, [online] 6(5), pp.682–688. Available at: <<https://doi.org/10.18517/ijaseit.6.5.938>> [Accessed 11 Feb. 2020].
- Berger, K., Cueli, A.B., Boddaert, S., Del Buono, S., Delisle, V., Fedorova, A., Frontini, F., Hendrick, P., Inoue, S., Ishii, H., Kapsis, C., Kim, J.-T., Kovacs, P., Chivelet, N.M., Laura, M., Machado, M., Schneider, A. and Wilson, H.R., 2018. *International definitions of “BIPV”*. [online] Available at: <<http://www.iea-pvps.org/index.php?id=501>> [Accessed 11 Feb. 2020].
- Boyle, G., 2012. Solar Photovoltaics. In: G. Boyle, ed. *Renewable Energy: Power of a Sustainable Future*, 3rd ed. United Kingdom: Oxford University Press. pp.75–113.
- Chew, K.W., 2015. *Study of Ventilation-Temperature Effect Due to Gaps Between Solar Panels and Roof on The Performance of PV Module*. Universiti Tunku Abdul Rahman.
- Chong, S.X., 2015. *Ventilation Study of PV Panels in Malaysia Climate: Forced Air Convection and Natural Convection Effect*. Universiti Tunku Abdul Rahman.
- Dash, P.K. and Gupta, N.C., 2015. Effect of Temperature on Power Output from Different Commercially available Photovoltaic Modules. *Journal of Engineering Research and Applications*, [online] 5(1), pp.148–151. Available at: <www.ijera.com> [Accessed 16 Feb. 2020].
- Gan, G., 2009a. Effect of air gap on the performance of building-integrated photovoltaics. *Energy*, [online] 34(7), pp.913–921. Available at: <<https://doi.org/10.1016/j.energy.2009.04.003>> [Accessed 20 Feb. 2020].
- Gan, G., 2009b. Numerical determination of adequate air gaps for building-integrated photovoltaics. *Solar Energy*, [online] 83(8), pp.1253–1273. Available at: <<https://doi.org/10.1016/j.solener.2009.02.008>> [Accessed 20 Feb. 2020].
- Goh, K.C., Goh, H.H., Yap, A.B.K., Masrom, M.A.N. and Mohamed, S., 2017. Barriers and Drivers of Malaysian BIPV Application: Perspective of Developers. *Procedia Engineering*, [online] 180, pp.1585–1595. Available at: <<https://doi.org/10.1016/j.proeng.2017.04.321>> [Accessed 21 Jan. 2020].

Ho, Z.X., 2015. *Ventilation- Temperature Effect on Diffrent Types of Roof Materials to A Photovoltaic Module*. Universiti Tunku Abdul Rahman.

IEC/TS61836, 2016. *Solar photovoltaic energy systems – Terms, definitions and symbols*. IEC/TS 61836. [online] IEC. Available at: <<https://webstore.iec.ch/publication/59630>> [Accessed 11 Feb. 2020].

Mertens, K., 2019. *Photovoltaics Fundamentals, Technology and Praticce*. 2nd ed. Steinfurt: Wiley.

REN21, 2019. *REN21 - 2019 Global Status Report*. [online] REN21. Available at: <<https://wedocs.unep.org/bitstream/handle/20.500.11822/28496/REN2019.pdf?sequence=1&isAllowed=y%0Ahttp://www.ren21.net/cities/wp-content/uploads/2019/05/REC-GSR-Low-Res.pdf>> [Accessed 11 Feb. 2020].

Ross, R.G., 1976. Interface Design Considerations For Terrestrial Solar Cell Modules. In: *Proceedings of the 12th IEEE Photovoltaic Specialists Conference*. [online] pp.801–806. Available at: <[https://www2.jpl.nasa.gov/adv_tech/photovol/ppr_75-80/Interface Des Consid_PVSC76.pdf](https://www2.jpl.nasa.gov/adv_tech/photovol/ppr_75-80/Interface_Des Consid_PVSC76.pdf)> [Accessed 18 Feb. 2020].

Salam, Z., Ramli, Z., Ahmed, J. and Amjad, M., 2015. Partial shading in building integrated PV system: Causes, effects and mitigating techniques. *International Journal of Power Electronics and Drive Systems*, 6(4), pp.712–722.

Skoplaki, E. and Palyvos, J.A., 2009. Operating temperature of photovoltaic modules: A survey of pertinent correlations. *Renewable Energy*, [online] 34(1), pp.23–29. Available at: <<https://doi.org/10.1016/j.renene.2008.04.009>> [Accessed 18 Feb. 2020].

Suruhanjaya Tenaga, 2019. *Malaysia Energy Statistics Handbook 2018*. [online] *Suruhanjaya Tenaga (Energy Commission)*. Putrajaya: Suruhanjaya Tenaga (Energy Commission). Available at: <<https://meih.st.gov.my/documents/10620/c7e69704-6f80-40ae-a764-ad0acf4a844d>> [Accessed 11 Feb. 2020].

Tenaga Nasional Berhad, 2020. *Pricing & Tariffs*. [online] Tenaga Nasional Berhad. Available at: <<https://www.tnb.com.my/residential/pricing-tariffs>> [Accessed 9 Sep. 2020].

Ye, Z., Nobre, A., Reindl, T., Luther, J. and Reise, C., 2013. On PV module temperatures in tropical regions. *Solar Energy*, [online] 88, pp.80–87. Available at: <<https://doi.org/10.1016/j.solener.2012.11.001>> [Accessed 18 Feb. 2020].

Zakaria, N.Z., Zainuddin, H., Shaari, S., Sulaiman, S.I. and Ismail, R., 2013. Critical factors affecting retrofitted roof-mounted photovoltaic arrays: Malaysian case study. In: *CEAT 2013 - 2013 IEEE Conference on Clean Energy and Technology*. [online] IEEE.pp.384–388. Available at: <<https://doi.org/10.1109/CEAT.2013.6775661>> [Accessed 24 Feb. 2020].

APPENDIX

APPENDIX A: Raspberry PI Data Logger Coding

PV Panel Operating Temperature Data Logger Coding

```

import time
import os
from datetime import datetime
from w1thermsensor import W1ThermSensor
import RPi.GPIO as GPIO
import sys
from urllib.request import urlopen

#myAPI = 'FSBNE3W21WTG88TN'
#baseURL = 'https://api.thingspeak.com/update?api_key={}'.format(myAPI)

def sensor():
    now = time.strftime("%H:%M:%S")
    sensor1 = W1ThermSensor(W1ThermSensor.THERM_SENSOR_DS18B20,
"0300a27921cf")
    sensor2 = W1ThermSensor(W1ThermSensor.THERM_SENSOR_DS18B20,
"0316a279197a")
    sensor3 = W1ThermSensor(W1ThermSensor.THERM_SENSOR_DS18B20,
"0300a2791b81")
    sensor4 = W1ThermSensor(W1ThermSensor.THERM_SENSOR_DS18B20,
"0300a279b374")
    sensor5 = W1ThermSensor(W1ThermSensor.THERM_SENSOR_DS18B20,
"0300a2799dfd")
    sensor6 = W1ThermSensor(W1ThermSensor.THERM_SENSOR_DS18B20,
"0300a2794446")
    sensor7 = W1ThermSensor(W1ThermSensor.THERM_SENSOR_DS18B20,
"0300a279399c")
    sensor8 = W1ThermSensor(W1ThermSensor.THERM_SENSOR_DS18B20,
"0300a2799d75")

```



```

temp1 = sensor1.get_temperature()
temp2 = sensor2.get_temperature()
temp3 = sensor3.get_temperature()
temp4 = sensor4.get_temperature()
temp5 = sensor5.get_temperature()
temp6 = sensor6.get_temperature()
temp7 = sensor7.get_temperature()
temp8 = sensor8.get_temperature()
f.write(str(now)+",")
f.write(str(temp1)+","+str(temp2)+ "," +str(temp3)+ ","+str(temp4)+
"+str(temp5)+ ","+str(temp6)+ ","+str(temp7)+ ","+str(temp8)+ ",")
#print("Temp                                     (Cel):
{ }'.format(temp1,temp2,temp3,temp4,temp5,temp6,temp7,temp8))
#conn = urlopen(baseURL +
"&field1={ }&field2={ }&field3={ }&field4={ }&field5={ }&field6={ }&field7
={ }&field8={ }".format(temp1,temp2,temp3,temp4,temp5,temp6,temp7,temp8
))
#print("Response :{ }".format(conn.read()))
#conn.close()

while True:
    now = datetime.now()
    year = str(now.year)
    month = str(now.month)
    day = str(now.day)
    hour = str(now.hour)

    exists_year = os.path.isdir('/home/pi/FYP2Data/PVT/'+year)
    if exists_year:
        pass
    else:
        os.chdir('/home/pi/FYP2Data/PVT/')
        os.mkdir(year)

```

```

exists_month = os.path.isdir('/home/pi/FYP2Data/PVT/'+year+'/'+month)
if exists_month:
    pass
else:
    os.mkdir('/home/pi/FYP2Data/PVT/'+year+')
    os.mkdir(month)

file = (day+"-"+month+"-"+year)
exists = os.path.isfile('/home/pi/FYP2Data/PVT/'+year+'/'+month+'/'+ file
+'.csv')
if exists:
    pass
else:
    f = open ('/home/pi/FYP2Data/PVT/'+year + '/' + month + '/' +file + '.csv',
'+a')
    f.write(", "+"\\n")

f.write("Time"+", "+"TempRefLUC"+", "+"TempRefRUC"+", "+"TempRefLB
C"+", "+"TempRefRBC"+", "+"TempExpLUC"+", "+"TempExpRUC"+", "+"Te
mpExpLBC"+", "+"TempExpRBC"+",")
    f.close

now = time.strftime("%H:%M:%S")
sec = int(time.strftime("%S"))

if (sec%30 == 0):
    f= open ('/home/pi/FYP2Data/PVT/'+year + '/' + month + '/' + file +
'.csv' ,'+a')
    f.write(", "+"\\n")
    sensor()
    f.close()
    time.sleep(5)

```

Ambient Temperature Data Logger Coding

```

import time
import os
from datetime import datetime
from w1thermsensor import W1ThermSensor
import RPi.GPIO as GPIO
import sys
from urllib.request import urlopen

#myAPI = 'EE5IEYXFPYZE1NNL'
#baseURL = 'https://api.thingspeak.com/update?api_key={}'.format(myAPI)

def sensor():
    now = time.strftime("%H:%M:%S")
    sensor = W1ThermSensor(W1ThermSensor.THERM_SENSOR_DS18B20,
"0416a02084ff")
    temp = sensor.get_temperature()
    f.write(str(now)+",")
    f.write(str(temp)+",")
    #print("Temp                                     (Cel):
 '{}'.format(temp1,temp2,temp3,temp4,temp5,temp6,temp7,temp8))
    #conn = urlopen(baseURL + "&field1={}".format(temp))
    #print("Response : {}".format(conn.read()))
    #conn.close()

while True:
    now = datetime.now()
    year = str(now.year)
    month = str(now.month)
    day = str(now.day)
    hour = str(now.hour)

    exists_year = os.path.isdir('/home/pi/FYP2Data/AT/'+year)

```

```

if exists_year:
    pass
else:
    os.chdir('/home/pi/FYP2Data/AT/')
    os.mkdir(year)

exists_month = os.path.isdir('/home/pi/FYP2Data/AT/'+year+'/'+month)
if exists_month:
    pass
else:
    os.chdir('/home/pi/FYP2Data/AT/'+year+')
    os.mkdir(month)

file = (day+"-"+month+"-"+year)
exists = os.path.isfile('/home/pi/FYP2Data/AT/'+year+'/'+month+'/'+ file
+'.csv')
if exists:
    pass
else:
    f = open ('/home/pi/FYP2Data/AT/'+year + '/' + month + '/' +file + '.csv',
'+a')
    f.write(",","\n")
    f.write("Time"+",","AmbientTempreature"+",")
    f.close

now = time.strftime("%H:%M:%S")
sec = int(time.strftime("%S"))

if (sec%30 == 0):
    f= open ('/home/pi/FYP2Data/AT/'+year + '/' + month + '/' + file +
'.csv', '+a')
    f.write(",","\n")
    sensor()

```

```
f.close()
```

```
time.sleep(5)
```

APPENDIX B: Result List for Average Operating Temperature of PV Panel in
A Day and Temperature Difference Between Reference PV panel and
Experimental PV Panel.

Table B.1: Average Operating Temperature of PV Panel in A Day and
Temperature Difference Between Reference PV panel = 12.5 cm and
Experimental PV Panel = 12.5 cm

Date	$T_{Avg,Ref} / ^\circ\text{C}$	$T_{Avg,Exp} / ^\circ\text{C}$	$\Delta T_{Avg} / ^\circ\text{C}$	% Difference / %
26/6/2020	42.6405	43.4974	0.8569	2.0097
27/6/2020	42.7366	43.5783	0.8417	1.9694
28/6/2020	41.9742	42.8992	0.9250	2.2036
29/6/2020	38.1664	38.9352	0.7688	2.0145
30/6/2020	42.39	43.2353	0.8453	1.9942
14/7/2020	41.5593	42.6060	1.0467	2.5186
15/7/2020	43.0211	44.2484	1.2273	2.8528
16/7/2020	39.0923	40.0432	0.9509	2.4324
17/7/2020	47.6625	49.2025	1.5400	3.2309
18/7/2020	44.8963	45.9006	1.0043	2.2370
$T_{Avg,Acc}$	42.4139	43.4146	1.0007	2.3593

Table B.2: Average Operating Temperature of PV Panel in A Day and
Temperature Difference Between Reference PV panel = 12.5 cm and
Experimental PV Panel = 10.5 cm

Date	$T_{Avg,Ref} / ^\circ\text{C}$	$T_{Avg,Exp} / ^\circ\text{C}$	$\Delta T_{Avg} / ^\circ\text{C}$	% Difference / %
8/7/2020	37.7316	38.4816	0.7500	1.9877
9/7/2020	35.6983	36.7379	1.0396	2.9123
10/7/2020	36.9275	37.524	0.5965	1.6153
11/7/2020	39.8768	41.067	1.1902	2.9848
12/7/2020	47.0345	48.8661	1.8316	3.8943
$T_{Avg,Acc}$	39.4537	40.5353	1.0816	2.7414

Table B.3: Average Operating Temperature of PV Panel in A Day and Temperature Difference Between Reference PV panel = 12.5 cm and Experimental PV Panel = 14.5 cm

Date	$T_{Avg,Ref} / ^\circ\text{C}$	$T_{Avg,Exp} / ^\circ\text{C}$	$\Delta T_{Avg} / ^\circ\text{C}$	% Difference / %
20/7/2020	49.741	49.9021	0.1611	0.3238
21/7/2020	52.1716	52.3504	0.1788	0.3427
22/7/2020	38.3061	38.3418	0.0357	0.0934
23/7/2020	38.4697	38.5255	0.0558	0.1449
24/7/2020	42.674	42.7194	0.0454	0.1064
$T_{Avg,Acc}$	44.2725	44.3678	0.0954	0.2154

Table B.4: Average Operating Temperature of PV Panel in A Day and Temperature Difference Between Reference PV panel = 12.5 cm and Experimental PV Panel = 16.5 cm

Date	$T_{Avg,Ref} / ^\circ\text{C}$	$T_{Avg,Exp} / ^\circ\text{C}$	$\Delta T_{Avg} / ^\circ\text{C}$	% Difference / %
26/7/2020	43.5691	43.3001	-0.2690	-0.6174
27/7/2020	37.0678	36.9615	-0.1063	-0.2868
28/7/2020	36.7684	36.7266	-0.0418	-0.1135
29/7/2020	40.2793	39.9998	-0.2795	-0.6939
30/7/2020	45.3858	45.0343	-0.3515	-0.7744
$T_{Avg,Acc}$	40.6141	40.4045	-0.2096	-0.5161

Table B.5: Average Operating Temperature of PV Panel in A Day and Temperature Difference Between Reference PV panel = 12.5 cm and Experimental PV Panel = 18.5 cm

Date	$T_{Avg,Ref} / ^\circ\text{C}$	$T_{Avg,Exp} / ^\circ\text{C}$	$\Delta T_{Avg} / ^\circ\text{C}$	% Difference / %
1/8/2020	44.3359	43.7455	-0.5904	-1.3316
2/8/2020	43.1392	42.6809	-0.4583	-1.0623
3/8/2020	39.6099	39.1351	-0.4748	-1.1985
4/8/2020	50.4378	49.8212	-0.6166	-1.2225
5/8/2020	44.2413	43.9369	-0.3044	-0.6881
$T_{Avg,Acc}$	44.3528	43.8639	-0.4889	-1.1023

Table B.6: Average Operating Temperature of PV Panel in A Day and Temperature Difference Between Reference PV panel = 12.5 cm and Experimental PV Panel = 20.5 cm

Date	$T_{Avg,Ref} / ^\circ\text{C}$	$T_{Avg,Exp} / ^\circ\text{C}$	$\Delta T_{Avg} / ^\circ\text{C}$	% Difference / %
7/8/2020	44.6819	44.192	-0.4899	-1.0963
8/8/2020	49.3906	48.7473	-0.6433	-1.3023
9/8/2020	47.3003	46.7643	-0.5360	-1.1330
10/8/2020	48.4381	47.9916	-0.4465	-0.9218
11/8/2020	43.2771	42.8041	-0.4730	-1.0928
$T_{Avg,Acc}$	46.6176	46.0999	-0.5177	-1.1106

APPENDIX C: Result List for Electricity Generated by PV Panel in A Day
and Electricity Generation Percentage Difference Percentage Difference
Between Reference PV panel and Experimental PV Panel.

Table C.1: Electricity Generated by PV Panels in a Day and Electricity
Generation Percentage Difference Between Reference PV panel = 12.5 cm and
Experimental PV Panel = 10.5 cm

Date	E_{Ref} / kWh	E_{Exp} / kWh	% Difference / %
8/7/2020	0.6673	0.689	3.2596
9/7/2020	0.6098	0.6288	3.1160
10/7/2020	0.6262	0.6459	3.1541
11/7/2020	0.6869	0.7118	3.6152
12/7/2020	1.0158	1.0563	3.9872
Total	3.6060	3.7318	3.4886

Table C.2: Electricity Generated by PV Panels in a Day and Electricity
Generation Percentage Difference Between Reference PV panel = 12.5 cm and
Experimental PV Panel = 14.5 cm

Date	E_{Ref} / kWh	E_{Exp} / kWh	% Difference / %
20/7/2020	1.0750	1.1278	4.9147
21/7/2020	1.2083	1.2753	5.5488
22/7/2020	0.6566	0.6798	3.5411
23/7/2020	0.6176	0.6428	4.0885
24/7/2020	0.7393	0.7749	4.8129
Total	4.2968	4.5006	4.7431

Table C.3: Electricity Generated by PV Panels in a Day and Electricity
Generation Percentage Difference Between Reference PV panel = 12.5 cm and
Experimental PV Panel = 16.5 cm

Date	E_{Ref} / kWh	E_{Exp} / kWh	% Difference / %
26/7/2020	0.8788	0.9193	4.5989
27/7/2020	0.658	0.6852	4.1287

28/7/2020	0.7236	0.75	3.6508
29/7/2020	0.7078	0.7324	3.4852
30/7/2020	0.9763	1.0218	4.6607
Total	3.9445	4.1087	4.1628

Table C.4: Electricity Generated by PV Panels in a Day and Electricity Generation Percentage Difference Between Reference PV panel = 12.5 cm and Experimental PV Panel = 18.5 cm

Date	E_{Ref} / kWh	E_{Exp} / kWh	% Difference / %
1/8/2020	1.0780	1.1288	4.7078
2/8/2020	0.9608	1.0048	4.5794
3/8/2020	0.7616	0.7933	4.1689
4/8/2020	1.2262	1.2930	5.4506
5/8/2020	0.9151	0.9590	4.1435
Total	4.9417	5.1729	4.6786

Table C.5: Electricity Generated by PV Panels in a Day and Electricity Generation Percentage Difference Between Reference PV panel = 12.5 cm and Experimental PV Panel = 20.5 cm

Date	E_{Ref} / kWh	E_{Exp} / kWh	% Difference / %
7/8/2020	1.0068	1.0547	4.7509
8/8/2020	1.2185	1.2844	5.4097
9/8/2020	0.9608	1.0058	4.6748
10/8/2020	1.173	1.2364	5.4064
11/8/2020	0.8347	0.8706	4.3031
Total	5.1836	5.4414	4.9734

APPENDIX D: List of Ross Coefficient Graphs between Experimental PV Panel and Reference PV Panel.

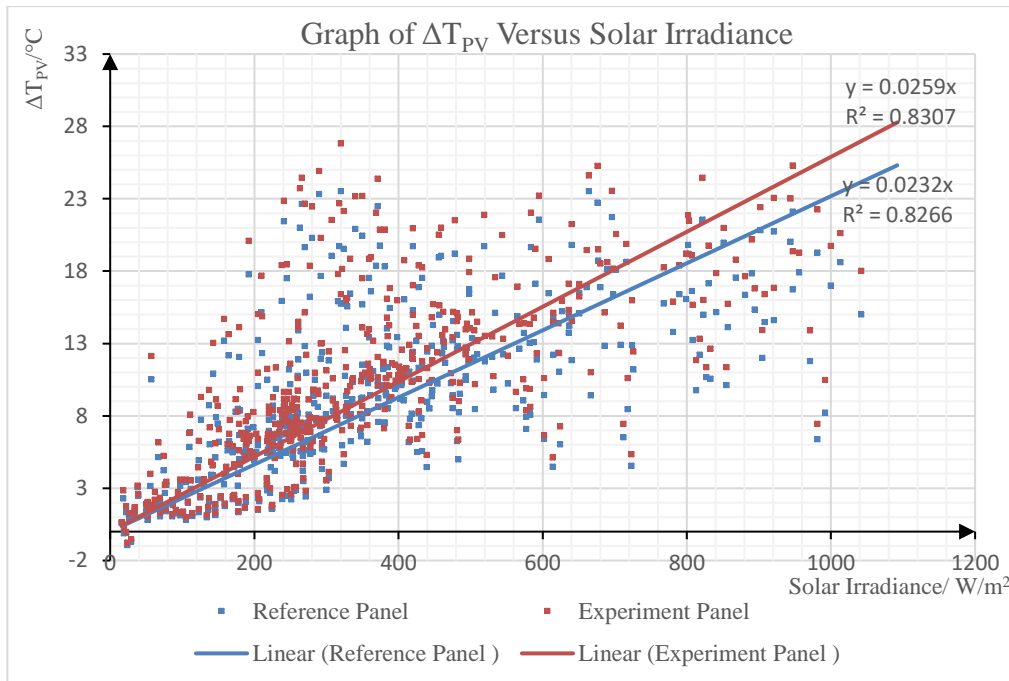


Figure D.1: Graph of ΔT_{PV} versus Solar Irradiance for Reference air gap = 12.5 cm and Experimental Air Gap = 10.5 cm.

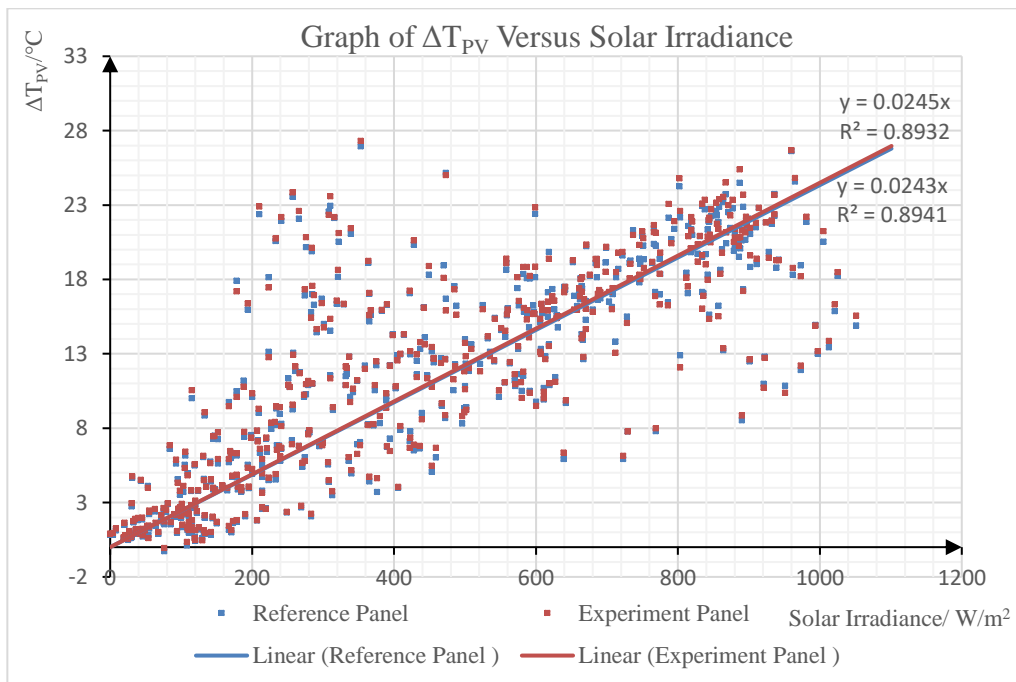


Figure D.2: Graph of ΔT_{PV} versus Solar Irradiance for Reference air gap = 12.5 cm and Experimental Air Gap = 14.5 cm.

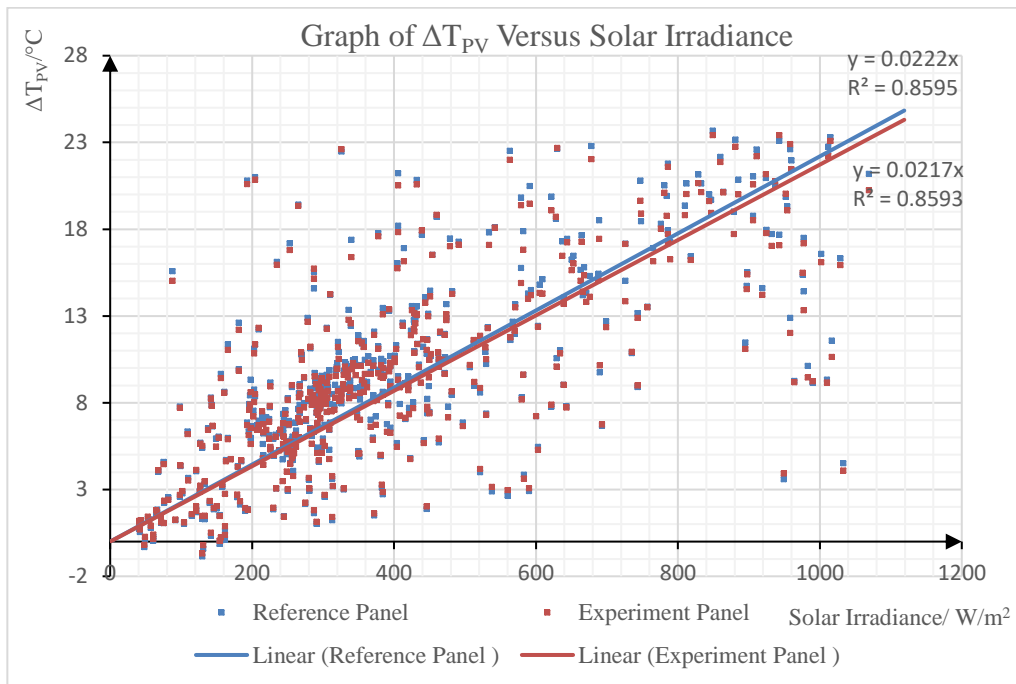


Figure D.3: Graph of ΔT_{PV} versus Solar Irradiance for Reference air gap = 12.5 cm and Experimental Air Gap= 16.5 cm.

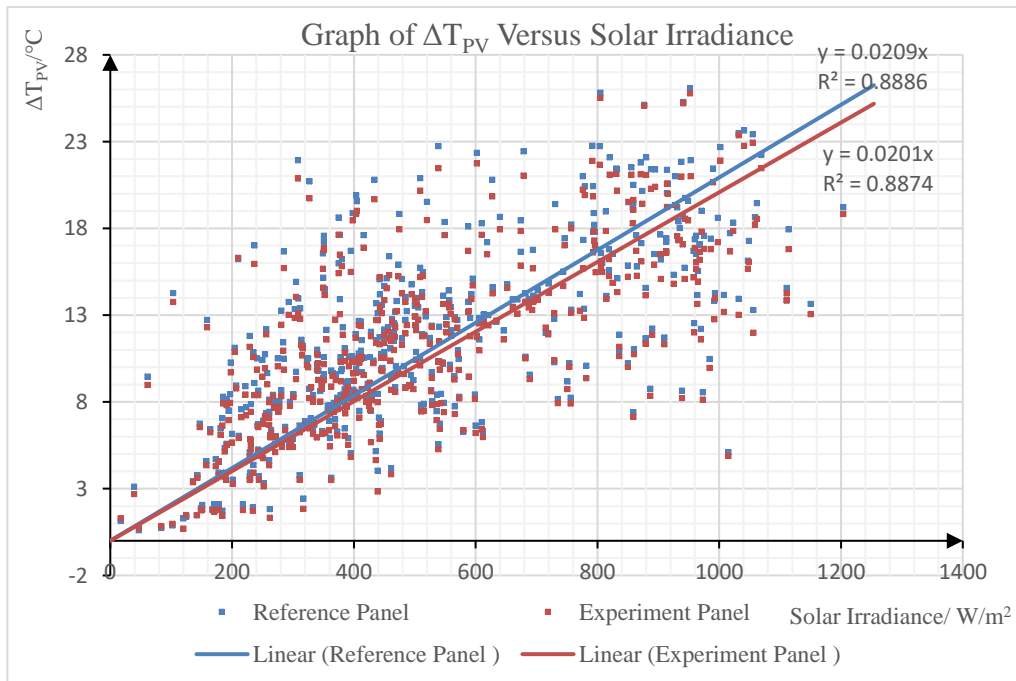


Figure D.4: Graph of ΔT_{PV} versus Solar Irradiance for Reference air gap = 12.5 cm and Experimental Air Gap= 18.5 cm.

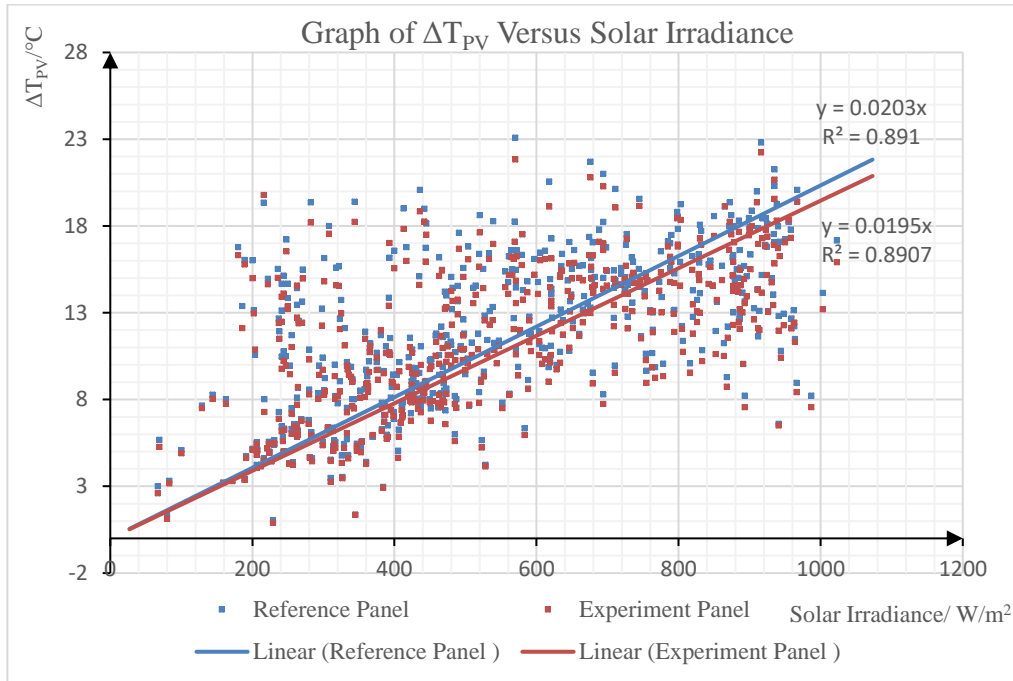


Figure D.5: Graph of ΔT_{PV} versus Solar Irradiance for Reference air gap = 12.5 cm and Experimental Air Gap= 20.5 cm.